Supporting Information

Enzymatic N- and C-protection in cyanobactin RiPP natural products

Debosmita Sardar, Yue Hao, Zhenjian Lin, Maho Morita, Satish K. Nair and Eric W. Schmidt

Table of Contents

SUPPORTING MATERIALS AND METHODS

Genes and cloning

Genes *truD* (GenBank ACA04490; from *Prochloron didemni*, a symbiont of tunicates) and *patG* protease/macrocyclase domain (GenBank AAY21156.1 amino acids 513-866; from *Prochloron didemni*) were described previously.[1, 2] The gene for RSI-TruD enzyme encoded the heterocyclase recognition sequence from PatE (GenBank AAY21154; from *Prochloron didemni*), RLTAGQLSSQLAELSEEALG,[3] fused at the N-terminus of *truD* followed by a tetra Gly-Ser spacer link. This fusion facilitates leader-independent heterocyclization of peptide substrates.

Genes *ageMTPT* (GenBank CCH92966; from *Microcystis aeruginosa* PCC 943) and *ageG* (CCH92964 amino acids 609-960; from *Microcystis aeruginosa* PCC 9432), with codons optimized for expression in *E. coli*, were obtained from Genscript. The *ageMTPT* gene was inserted into pET15 with a N-terminal histidine tag and *ageG* into LIC cloning vector from Addgene with N-terminal histidine and maltose binding protein tags. The wild-type *ageMTPT* homolog from *Oscillatoria nigro-viridis* PCC 7112 (GenBank AFZ08007) was amplified by PCR from genomic DNA, and inserted into pET28 after the N-terminal His-tag, but the protein failed to express in our hands.

Protein expression and purification

RSI-TruD, AgeMTPT and AgeG were expressed in *E. coli* R2D-BL21(DE3). A seed culture was grown overnight at 30°C in 2 × YT media, and an aliquot (10 mL) was used to inoculate each liter of 2 × YT media. The cultures were grown at 30°C until OD_{600} = 0.6, followed by addition of IPTG (0.1 mM) and overnight growth at 18°C. The cells were harvested by centrifugation. Cell pellets were resuspended in lysis buffer (50 mM Tris, 200 mM NaCl, 10 mM imidazole, 5% glycerol, pH 7.5), stirred for 1 h with lysozyme (600 μg mL^{-1}), and sonicated to disrupt cells. After centrifugation, the supernatant was filtered and purified using Ni-NTA (Qiagen) affinity chromatography. The loaded resin was washed twice (1 M NaCl, 30 mM imidazole, pH 8.0), and proteins were eluted (1 M NaCl, 200 mM imidazole, pH 8.0). The eluates were analyzed by SDS-PAGE (Figure S19), dialyzed (25 mM HEPES, 500 mM NaCl, pH 8.0) at 4°C for 1-2 days, and stored as flash-frozen 10% glycerol aliquots at -80°C.

Substrate synthesis

The peptides **3** and **a**-**j** were synthesized using a resin method, purified, and analyzed by mass spectrometry (MS) at the University of Utah DNA/Peptide Synthesis Core Facility. Substrate **k** was chemically synthesized by the Hantzsch reaction. The adenosine analogs **5.1**-**5.3** (Figure S6) were obtained from Sigma-Aldrich. The substrate **8** was obtained based on a method described previously.[3] RSI-TruD and a cyanobactin N-terminal protease PatA were used on peptide **a** to produce **8** in reaction mixtures.

Analysis of reaction products

High-performance liquid chromatography-electrospray ionization MS (HPLC-ESI-MS) was performed using a Micromass Q-TOF Micro Mass Spectrometer (Waters) or a Micromass Quattro-II (Waters) instrument in positive ion mode, using an analytical Agilent Eclipse XDB-C4 column (4.6 × 150 mm, 5 μm) with a linear gradient of 1%-99% B over 20 m, where the mobile phase comprised solvent A (Optima LC-MS grade water with 0.05% formic acid) and solvent B (Optima LC-MS grade acetonitrile). Relative abundance of each intermediate species (**1** to **10**) if described, was calculated as a function of peak area, which is an absolute value obtained from the integration of the displayed mass peak from the total ion chromatogram of the mass spectrum. The relative percentage of product formation, if described, was calculated based on the integrated area peaks of substrate and product. If graphically presented, each data point is an average of duplicates, and error bars represent standard deviation. Each reaction described was performed at least in quadruplicate. A summary of substrates, intermediates, products, and percent yields is given in Table S1, and the corresponding mass of each species described in this study is listed in Table S2.

High-resolution MS (HRMS) of **1** was performed at the University of Utah Mass Spectrometry Core Facility in a maXis-II ETD Q-ToF instrument (Bruker) operated at 80.000 resolving power. Nuclear Magnetic Resonance (NMR) spectroscopy was performed on a Varian INOVA 500 (^{1}H 500 MHz, ^{13}C 125 MHz) NMR spectrometer with a 3 mm Nalorac MDBG probe.

RSI-TruD heterocyclization reaction

Peptide heterocyclization was performed using RSI-TruD in reaction mixtures containing Tris pH 7.5 (50 mM), $MgCl_2$ (5 mM), ATP (1 mM), DTT (5 mM), enzyme (1 μM) and substrate **3** (50 μM). Products were analyzed by HPLC-ESI-MS based upon loss of 18 Da corresponding to loss of water from the Pro-Cys amide bond. Reactions were incubated at 37°C for 1 h, leading to a yield of >98%. Heterocyclization also occurred in the absence of DTT with a lower yield of >61% in a 1 h reaction (Figure S2-A) and >95% yield after 2 h.

AgeMTPT methyl-prenyl transfer reactions

Reactions were done in Tris pH 7.5 (50 mM), $MgCl_2$ (5 mM), substrate (50 μM) and enzyme (2-5 μM). Reactions used dimethylallyl pyrophosphate (DMAPP, 5 mM) as the isoprene donor (chemically synthesized as described previously),[4] and/or *S*-adenosyl methionine (SAM, 5-10 mM) as the methyl donor (Sigma Aldrich). Negative control reaction for prenyl-methyl transfers was done in the absence of DMAPP, SAM and/or enzyme. Products were analyzed by HPLC-ESI-MS based upon addition of 68 Da or 14 Da, corresponding to addition of prenyl or methyl group, respectively. Reactions were typically incubated at 37°C for up to 2 h for prenyl transfer and up to 18 h for methyl transfer. The prenyl transfer reaction was efficient in that a yield of 78% was observed within 15 m of reaction, whereas the methyl transfer was slower with a yield of 60% observed after an 18 h reaction (Figure S2-B, D)

AgeG and PatG protease reactions

Reactions were done in in Tris pH 7.5 (50 mM), $MgCl_2$ (5 mM), substrate (50 μM) and protease (5-10 μM). Products were analyzed by HPLC-ESI-MS based upon loss of amino residues after proteolysis. Reactions were typically incubated at 37°C for up to 2 h or 18 h (or longer). AgeG (10 μM) proteolysis on **5** showed 80% yield of **6** after 2 h (Figure S2-C), whereas PatG (10 μM) was less efficient with a 31% yield of **6** after 24 h (Figure S15). AgeG (10 μM) proteolysis on **4** showed <10% yield of **4a** after 2 h (Figure S7). Longer reaction time points led to accumulation of a degradation product of **4** with loss of N-terminal Phe ($[M+H]^+$ 713.3 Da). PatG (10-20 μM) did not react with **4** in the same time scale (Figure S17) and longer reaction time points led to accumulation of the same degradation product $[M+H]^+$ 713.3 Da. For reactions with **8**, PatG/AgeG (10 μM) was added to reaction mixtures containing **8** in Tris buffer pH 7.5 (50 mM) and $MgCl_2$ (5 mM) at 37°C for 24 h. PatG converted **8** to **9** with >95% yield whereas AgeG converted **8** to **10** with 25% yield (Figures 3 and S18-A). A reaction with AgeG was made to proceed till 72 h and no cyclic product **9** was observed (Figure S18-B).

Competition experiments to determine substrate selectivity

(a) AgeMTPT vs AgeG on substrate **4**: Substrate **4** (50 μM) in Tris buffer pH 7.5 (50 mM), $MgCl_2$ (5 mM), AgeMTPT (1 μM)/DMAPP (5 mM) and AgeG (10 μM) were incubated at 37°C for 2 h. The experiment was designed to push the reaction through route II, by using a 10-fold excess of AgeG.

(b) AgeMTPT on substrate **6** vs **6a**: An equimolar amount of **6** and **6a** (50 μM) was subjected to AgeMTPT (5 μM), SAM (5 mM), $MgCl_2$ (5 mM) in Tris buffer pH 7.5 (50 mM) at 37°C for 45 m.

Synthesis of compound 7

Compound **3** (300 μM) and RSI-TruD (1 μM) were mixed in multiple 1.0 mL reaction mixtures containing Tris pH 7.5 (50 mM), $MgCl_2$ (5 mM), ATP (1 mM) at 37°C for 2 h. Each 1.0 mL mixture was dried down to ~300 μL under vacuum, followed by addition of AgeMTPT (2 μM) and DMAPP (5 mM). After 2 h at 37°C, the reaction mixture was treated with AgeG (5 μM) and left at 37°C for 20 h. Each reaction till this step proceeded to >95% completion. Subsequently, AgeMTPT (2 μM) and SAM (7 mM) were added, and the reaction mixture was left overnight at 37°C. The methyl transfer reaction was not complete and a purification step over a C18 resin plug was performed to isolate the compound **7**. SAM was removed using 40% (aq.) acetonitrile, non-methylated **5** was removed with 70% acetonitrile (aq.) and **7** was obtained in the 80%-90% acetonitrile (aq.) fraction, which was dried under vacuum. If necessary, a further HPLC purification was performed using a LaChrom Elite Hitachi system with a semi-preparative Jupiter C4 column (250 cm × 10 mm, 5 μm) in a linear gradient of 99% H_2O/5% ACN to 100% ACN over 40 min at a flow-rate of 2.5 ml m^{-1}. See Figure S12 and Table S3 for a detailed spectral data.

NMR characterization of 7

Purified **7** presented a mixture of two isomers (3:1 ratio in the ^{1}H NMR spectrum), which were traced to isomerization of the Pro amide. Analysis of the 2D NMR spectra, including COSY, HSQC, and HMBC in DMSO-d_6 (Figure S12), allowed for the complete spectroscopic assignment of a methoxyl group, an isoprene group and four amino acids residues (Phe (2), Pro, and Cys-derived thiazoline). An HMBC correlation from H-1 to C-2 indicated the presence of a methyl ester at the C-terminal of the cysteine-thiazoline residues. The NOESY correlation between 18-NH and H-28,27 indicated that the isoprene group was at the N-terminal Phe. Other HMBC correlations confirmed the Pro-thiazoline sequence. Most residues showed two sets of ^{1}H NMR signals, with the exception of Phe2, which had very broad (averaged) peaks (11-NH, H-11 and H-12). This was attributed to isomerization of the Phe-Pro amide bond. For chemical shift assignments, see Table S3.

Oxidation reactions to produce 1 and 6a

Three different methods were used, described as follows:[5-7]

1) MnO_2 method:[5] **7** (500 µg) was dissolved in of anhydrous DMSO (0.25 mL), and activated MnO_2 (3 mg) was added to the solution. The mixture was stirred at 150 rpm at 30°C for 72-96 h. By HPLC-ESI-MS, the reaction to **1** went to >80% completion (Figure S11). A similar method was used to oxidize **6** to **6a**, and the oxidation to **6a** went to completion. The MnO_2 was removed by centrifugation and washed 3x with methanol (1 mL). The DMSO/methanol fractions were combined and dried under vacuum. Further HPLC purification led to a series of degradation products in which only insignificant amounts of **1** could be identified. To test whether this degradation was due to the specific reaction conditions, two other methods were tried, as described.

2) DDQ/DCM method:[6] Molecular sieves (4 Å, 0.5 mg) were added to a solution of **7** (1 mg) in dichloromethane (200 µL). The mixture was stirred at room temperature for 10 m, and 2,3-dichloro-5,6-dicyano-1,4-benzoquinone (DDQ, 0.6 mg) was added. The mixture was stirred overnight under argon at room temperature. The reaction went to completion, but >50% of product carried an additional oxidation of +16 Da (591.2 Da $[M+H]^+$), which could be attributed to sulfoxide (Figure S11). The reaction mixture was quenched with 10% NaOH (300 µL) and extracted using 3x chloroform (300 µL) to yield an extract containing **1**. As with method (1) above, the product completely degraded during further purification.

3) K_2CO_3/DMF:[7] Molecular sieves (4 Å, 1 mg) and K_2CO_3 (1.0 mg) were added to a solution of **7** (500 µg) in anhydrous DMF (500 µL). The mixture was stirred at 80ºC for 6 h. The reaction went to >90% completion (HPLC-ESI-MS) (Figure S11). Molecular sieves were removed by centrifugation, and the DMF was dried to yield the product containing **1**. For purification, an HPLC system (LaChrom Elite, Hitachi) with a semi-preparative Jupiter C4 column (250 cm × 10 mm, 5 µm) was used in a linear gradient of 5%-100% acetonitrile in water over 40 m at a flow-rate of 2.5 ml m^{-1}. The compound **1** was found to be an extremely strong binder to the C4/C18 column and not stable upon purification.

SUPPORTING TABLES

Table S1. Enzymatic reactions performed in this study.

Substrate	Prenylation by AgeMTPT	Methylation by AgeMTPT	Proteolysis by AgeG (A) or PatG (P)
3, FFPCSYD	**3a**, 77.3% (t = 0.25 h)[a]	NR[b]	NR
4, FFPC*SYD	**5**, 78.5% (t = 0.25 h) **5**, >95% (t = 1 h)	NR	A[c]: **4a**, <10% (t = 2 h) P[d]: NR
a, LAELSEEAL-GGVDASTSIAPFCSYD	NR	NR	—[e]
b, LAELSEEAL-GGVDASTSIAPFC*SYD	NR	NR	—
c, TSIAPFPSYDD	NR	NR	—
d, AITFCAYDGE	NR	NR	—
e, AITFC*AYDGE	NR	NR	—
f, AITFCGVDAS	NR	NR	—
g, CITFC	NR	NR	—
h, CITFCA	NR	NR	—
i, CITFCAYDGE	NR	NR	—
j, CITFC*AYDGE	NR	NR	—
k, boc-GC*	—	NR	—
5, C_5H_9-FFPC*SYD	NR	NR	A: 80% (t = 2 h) P: <1% (t = 2 h) P: 35% (t = 48 h)
5.1, SAM	**5.1a**, <5% (t = 18 h)	—	—
5.2, adenosine	**5.2a**, <5% (t = 18 h)	—	—
5.3, adenine	**5.3a**, <5% (t = 18 h)	—	—
6, C_5H_9-FFPC*	NR	**7**, 60% (t = 18 h)	—
6a, C_5H_9-FFP-thiazole	NR	NR	—
8, TSIAPFC*SYD	NR	NR	A: **10**, 25% (t = 24 h) P: **9**, >95% (t = 24 h)

a. Product, % yield (reaction duration)
b. NR, no reaction
c. A, AgeG reaction
d. P, PatG reaction
e. —, reactions not attempted in this study
(note that PatG can proteolyze/cyclize **b**, **c**, **e** and **j**, as reported in an earlier study) [3]

Table S2. Expected molecular mass (*m/z*) of ions of species **1-10** observed in this study.

Compound	$[M+H]^+$
1	575.3
3	878.3
3a	946.4
4	860.3
4a	495.2
5	928.4
6	563.3
6a	561.3
7	577.3
8	1084.5
9	702.3
10	720.3

Table S3. NMR chemical shift assignments for compound **7** (see Figure S12).

	Conformer 1 (major)		**Conformer 2 (minor)**	
Position	**^{1}H NMR**	**^{13}C NMR**	**^{1}H NMR**	**^{13}C NMR**
1	3.71 s	52.8 CH_3	3.65 s	52.8 CH_3
2		171.3 C		170.9 C
3	5.14 dd (9.0, 9.0)	78.3 CH	5.01 dd (9.0, 9.0)	78.2 CH
4	3.57 m, 3.42 m	34.9 CH_2	3.47 m, 3.58 m	36.0 CH_2
5		175.7 C		175.0 C
6	4.81 m	59.0 CH	4.26 m	58.9 CH
7	2.12 m, 1.93 m	30.8 CH_2	1.83 m	32.6 CH_2
8	1.96 m	24.8 CH_2	1.72 m	22.4 CH_2
9	3.70 m, 3.60 m	47.3 CH	3.43 m, 3.29 m	46.5 CH
10		171.3 C		171.3 C
11	3.05 m	58.4 CH	3.05 m	58.4 CH
11-NH	8.32 brs		8.32 brs	
12	2.38 m, 2.65 m	40.9 CH_2	2.38 m, 2.65 m	40.9 CH_2
13-16	7.08-7.30 m	126.3-130.3	7.08-7.30 m	126.3-130.3
17		174.7 C		
18	4.78 m	51.5 CH	4.62 m	51.7 CH
18-NH	8.23 d (8.1)		8.17 d (8.1)	
19	3.02 m, 2.82 m	37.6 CH_2	2.82 m	40.0 CH_2
20-23	7.08-7.30 m	126.3-130.3	7.08-7.30 m	126.3-130.3
24		54.9 C		54.9 C
25	5.28 dd (17.8, 10.8)	146.3 CH	5.28 dd (17.8, 10.8)	146.3 CH
26	4.70 d (10.8), 4.75 d (17.8)	112.2 CH_2	4.70 d (10.8), 4.75 d (17.8)	112.2 CH_2
27	0.80 s	27.9 CH_3	0.77 s	26.0 CH_3

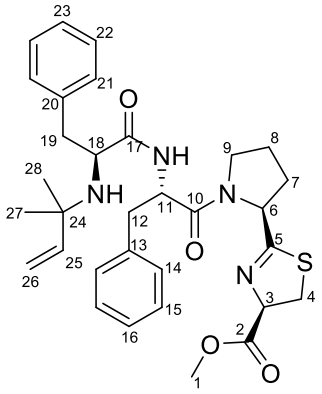

SUPPORTING FIGURES

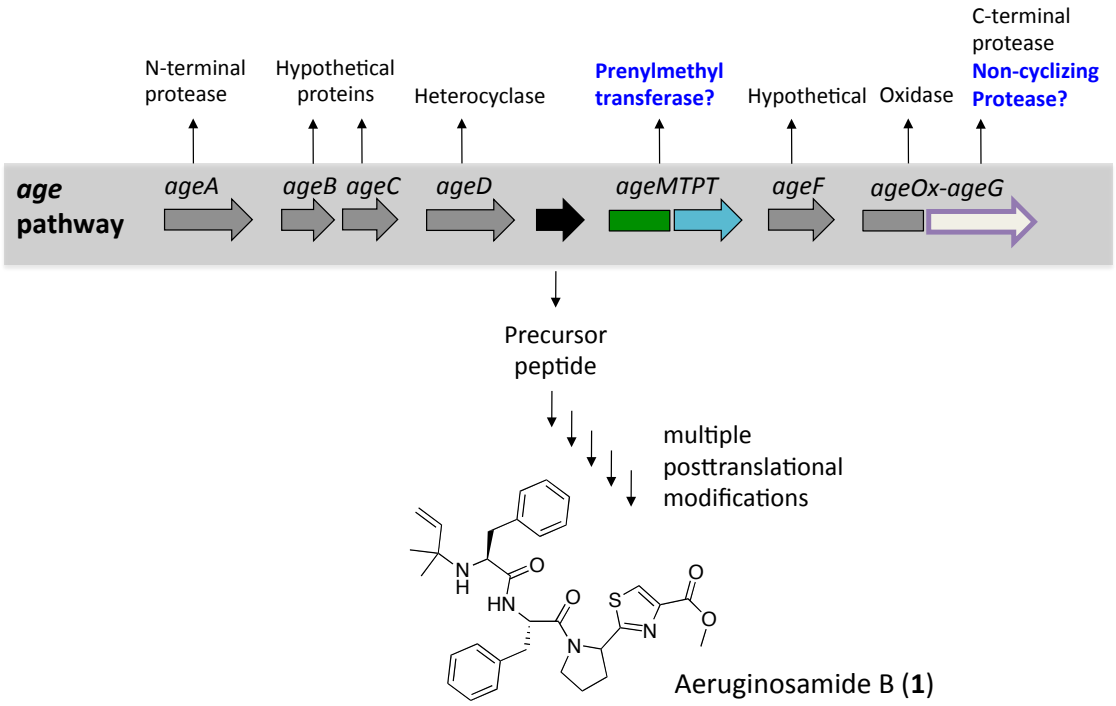

Figure S1. The cyanobactin pathway *age* to aeruginosamide B (**1**). The precursor peptide (black) is converted to the final natural product **1** by a series of posttranslational enzymes (grey/colored). The *age* pathway encodes two non-canonical cyanobactin enzymes AgeMTPT (putative prenyl-methyl transferase) and AgeG (putative linearizing protease).

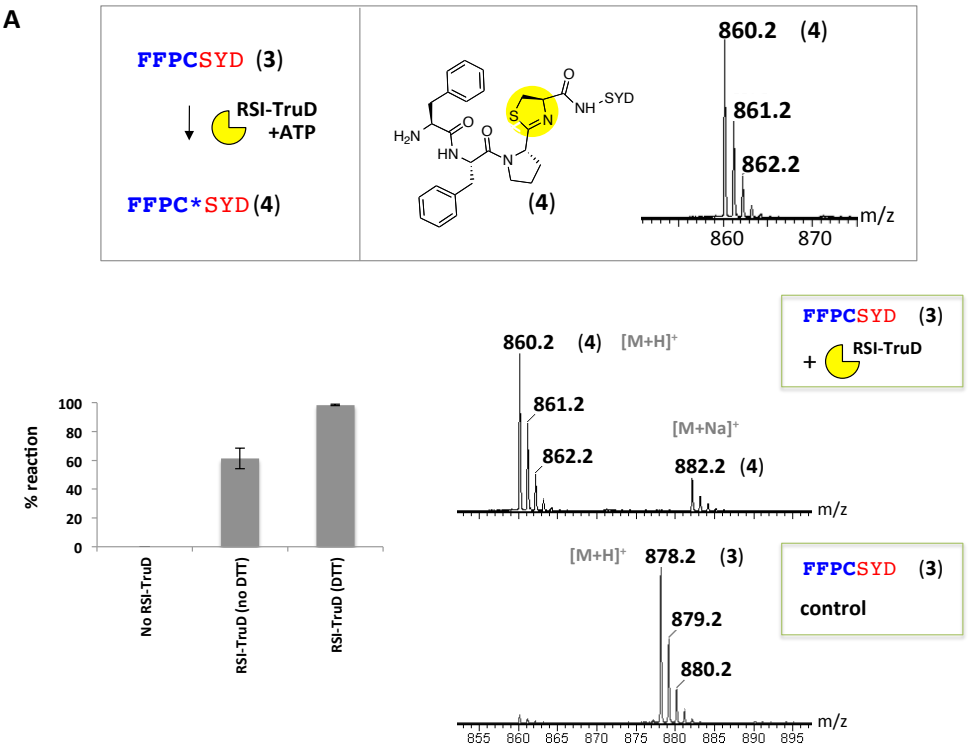
A
FFPCSYD (3)
RSI-TruD
+ATP
FFPC*SYD (4)
(4)
860.2 (4)
861.2
862.2
m/z
860
870
% reaction
100
80
60
40
20
0
No RSI-TruD
RSI-TruD (no DTT)
RSI-TruD (DTT)
FFPCSYD (3)
+ RSI-TruD
860.2 (4) [M+H]+
861.2
862.2
[M+Na]+
882.2 (4)
m/z
[M+H]+ 878.2 (3)
879.2
880.2
FFPCSYD (3)
control
855 860 865 870 875 880 885 890 895

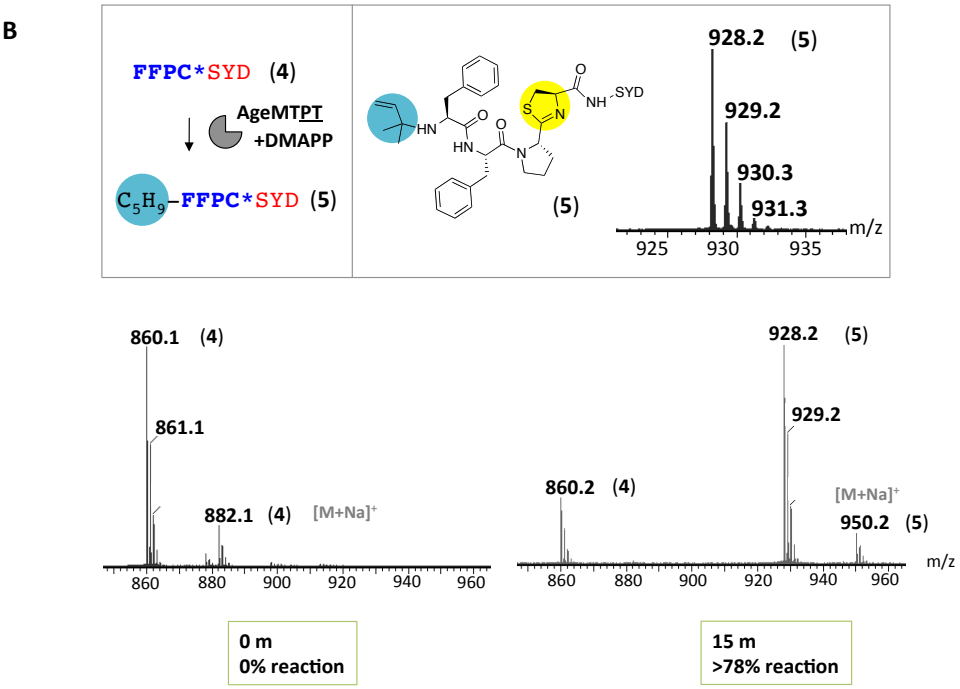
B
FFPC*SYD (4)
AgeMTPT
+DMAPP
C5H9–FFPC*SYD (5)
(5)
928.2 (5)
929.2
930.3
931.3
m/z
925
930
935
860.1 (4)
861.1
882.1 (4) [M+Na]+
860
880
900
920
940
960
928.2 (5)
929.2
860.2 (4)
[M+Na]+
950.2 (5)
m/z
0 m
0% reaction
15 m
>78% reaction

C

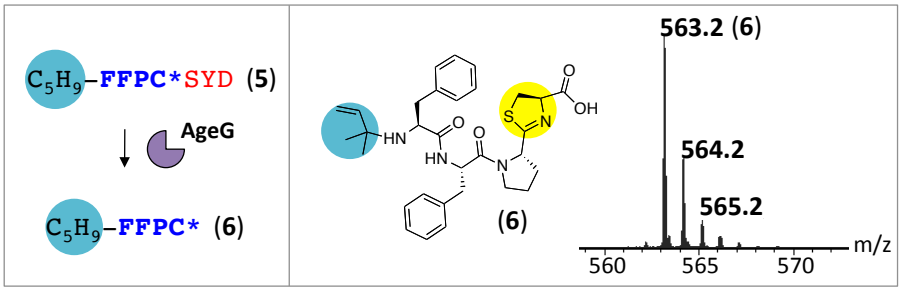

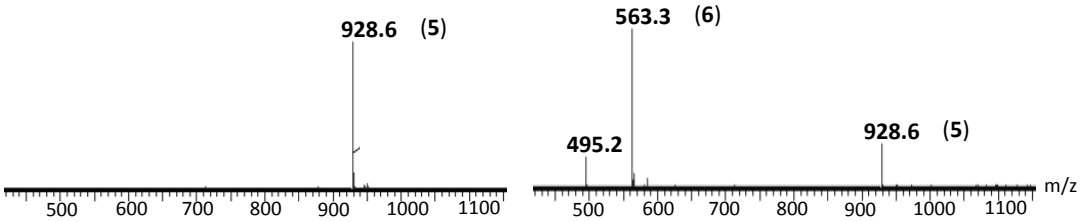

0 m
0% reaction

2 h
80% reaction

D

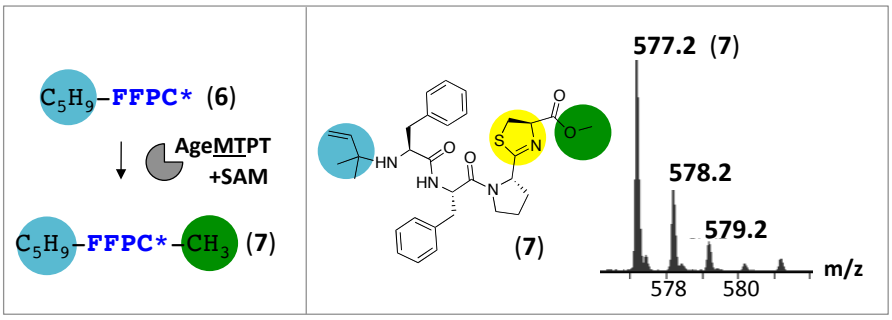

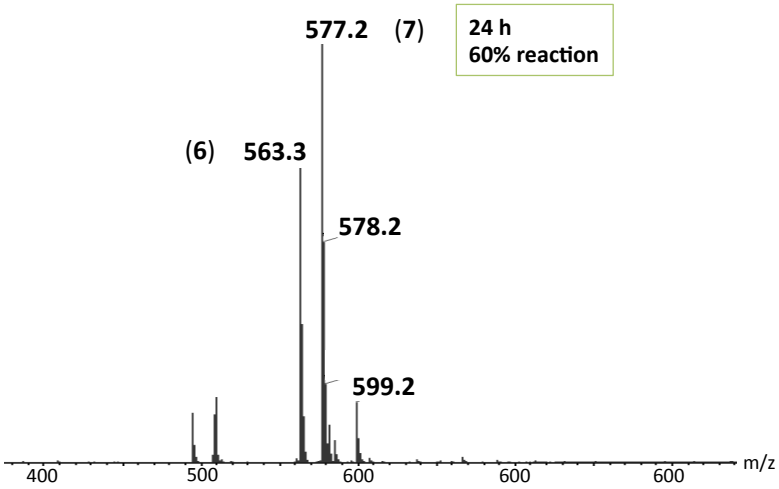

24 h
60% reaction

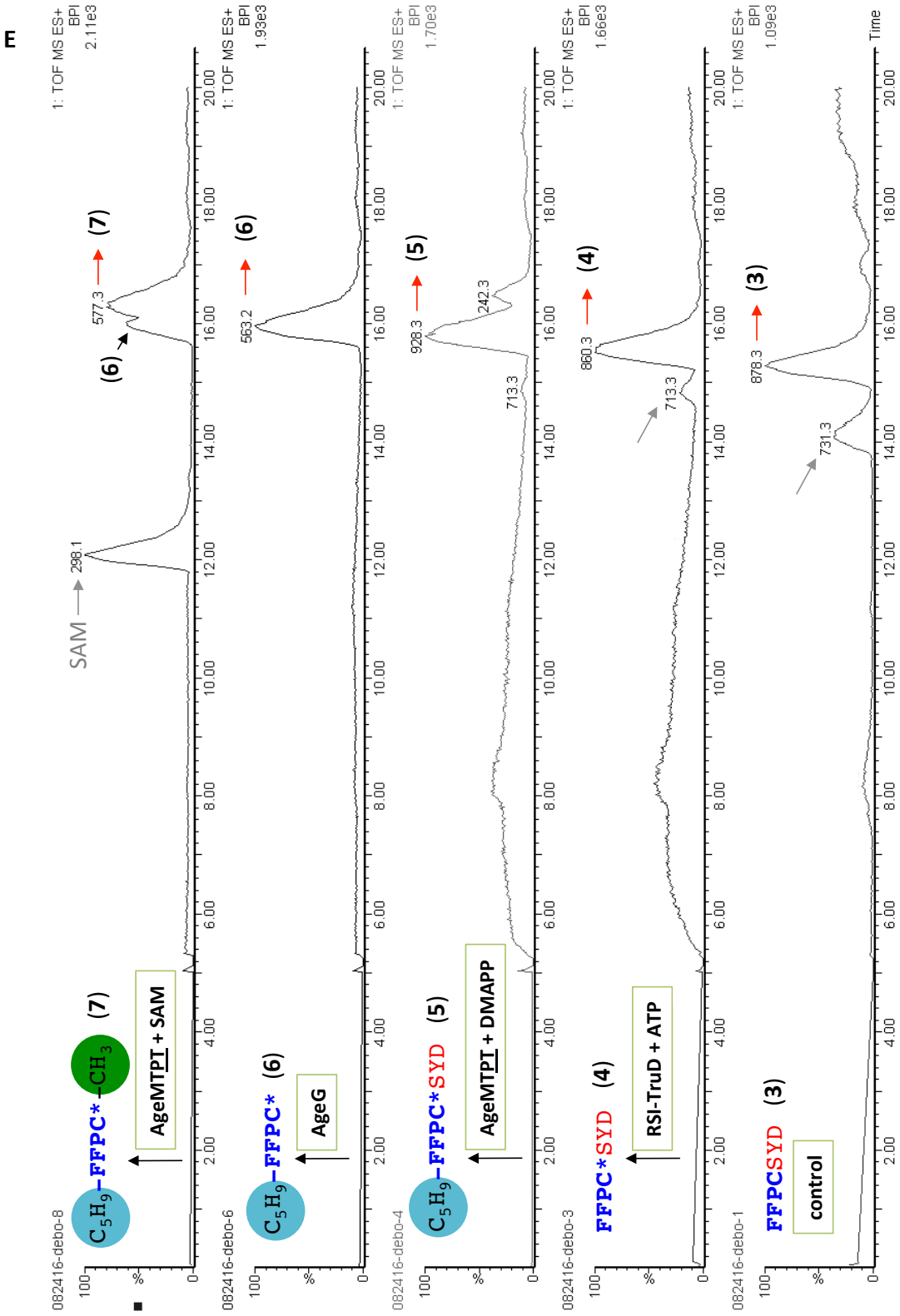
E
082416-debo-8
1: TOF MS ES+
BPI
2.11e3
C5H9–FFPC*–CH3 (7)
AgeMTPT + SAM
SAM
298.1
(6)
577.3
(7)
082416-debo-6
1: TOF MS ES+
BPI
1.93e3
C5H9–FFPC* (6)
AgeG
563.2
(6)
082416-debo-4
1: TOF MS ES+
BPI
1.70e3
C5H9–FFPC*SYD (5)
AgeMTPT + DMAPP
928.3
(5)
242.3
713.3
082416-debo-3
1: TOF MS ES+
BPI
1.66e3
FFPC*SYD (4)
RSI-TruD + ATP
860.3
(4)
713.3
082416-debo-1
1: TOF MS ES+
BPI
1.09e3
FFPCSYD (3)
control
878.3
(3)
731.3
Time

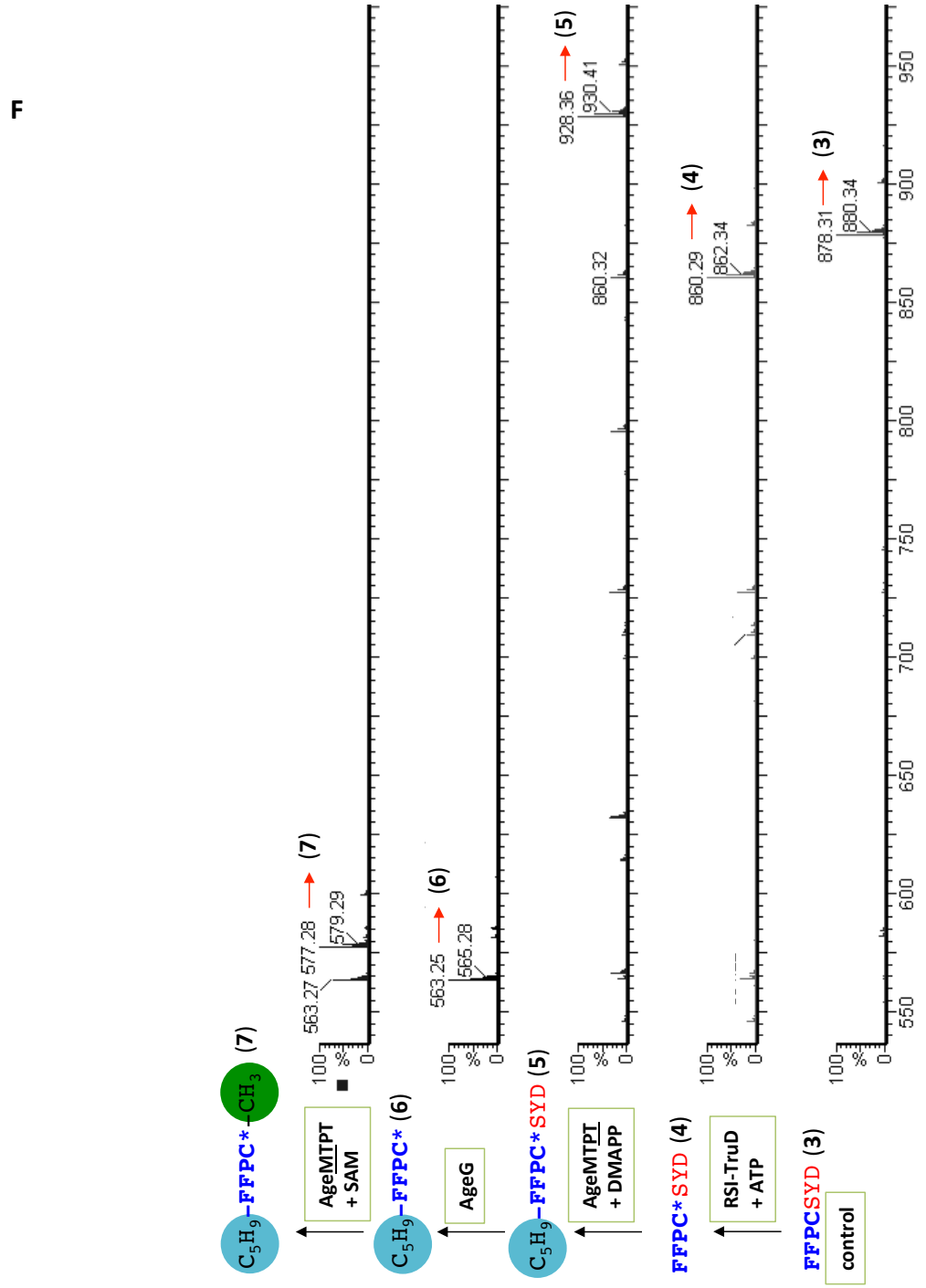

Figure S2. Posttranslational enzymatic reactions. (A) Heterocyclization (yellow circle) of **3** by RSI-TruD. (B) Prenylation (blue) of **4** by AgeMTPT. (C) Proteolysis of **5** by AgeG. (D) Methylation (green) of **6** by AgeMTPT. (E) Typical raw HPLC-ESI-MS chromatograms of crude reaction mixtures in the synthesis of **7** from **3**. Grey arrows indicate degradation product of **3** and **4** with loss of first Phe residue. (F) Raw integrated MS spectra from the chromatograms shown in (E). Red arrows indicate initial substrate **3** and subsequent products **4**, **5**, **6** and **7**. For NMR spectra of **7**, see Figure S12. For reaction conditions, see Supporting Methods.

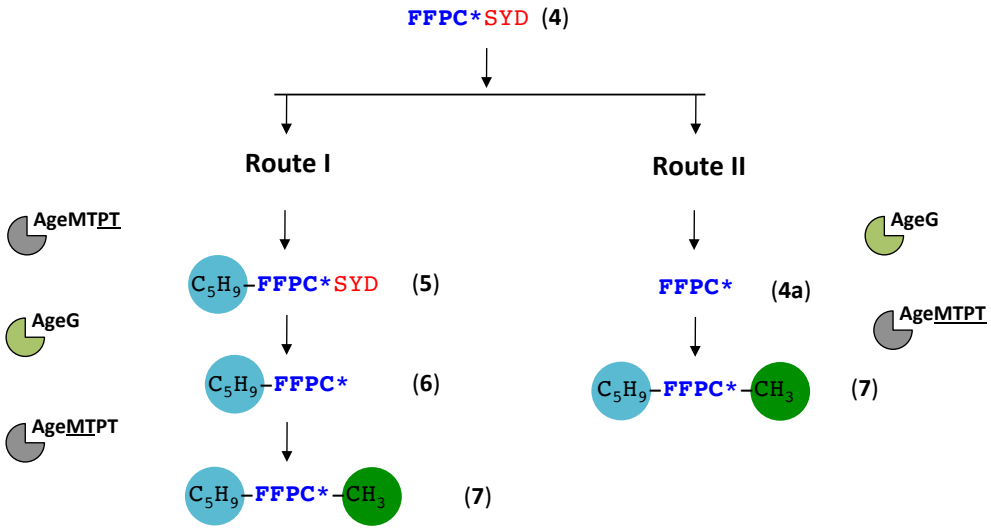

Figure S3. Two possible biosynthetic routes. In route I, **4** is first prenylated by AgeMTPT, followed by proteolysis by AgeG and subsequent methylation by AgeMTPT. In route II, **4** would be first proteolysed by AgeG, followed by methylation and prenylation by AgeMTPT.

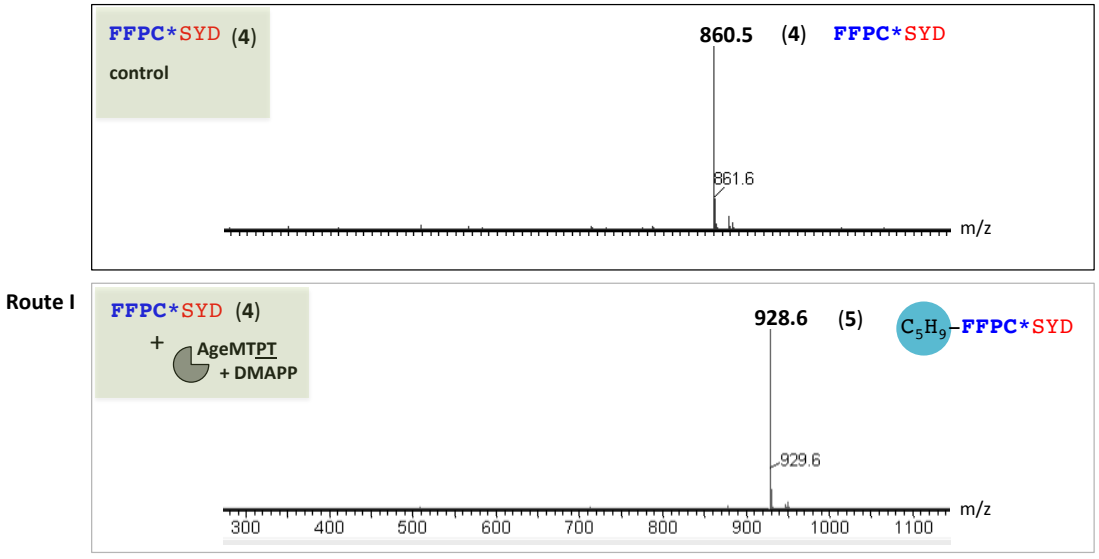

Figure S4. Fate of **4** through route I. Bottom: the mass spectrum of reaction of **4** with AgeMTPT (2 µM), DMAPP (5 mM) in Tris buffer pH 7.5 (50 mM) and $MgCl_2$ (5 mM) at 37°C for 2 h, leading to complete conversion to the singly prenylated product **5**, compared to control (top).

A

(a) LAELSEEALGGVDASTSIAPFCSYD
(b) LAELSEEALGGVDASTSIAPFC*SYD
(c) TSIAPFPSYDD
(d) AITFCAYDGE
(e) AITFC*AYDGE
(f) AITFCGVDAS
(g) CITFC
(h) CITFCA
(i) CITFCAYDGE
(j) CITFC*AYDGE

B

FFPCSYDD = *Microcystis* (AgeMTPT)

FFPVCSYDG = *Microcystis*
FICSVDG = *Oscillatoria*
FVPCCSYDD = *Planktothricoides*

C

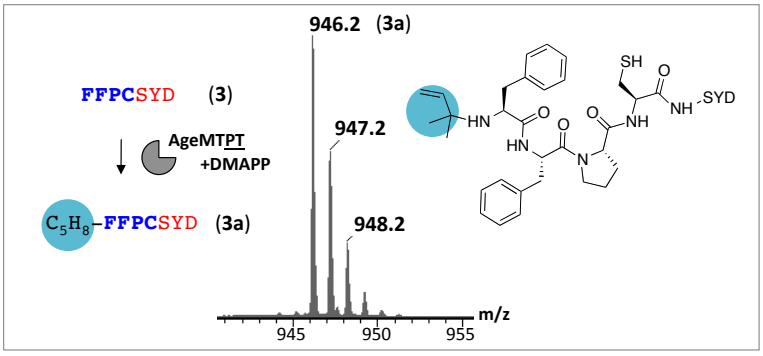

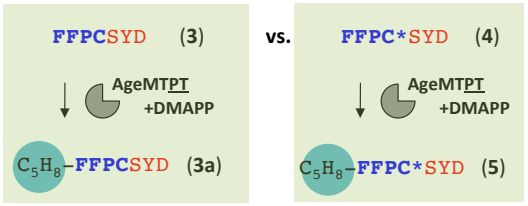

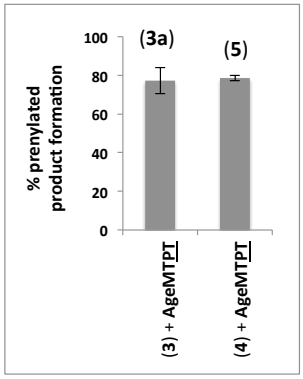

D

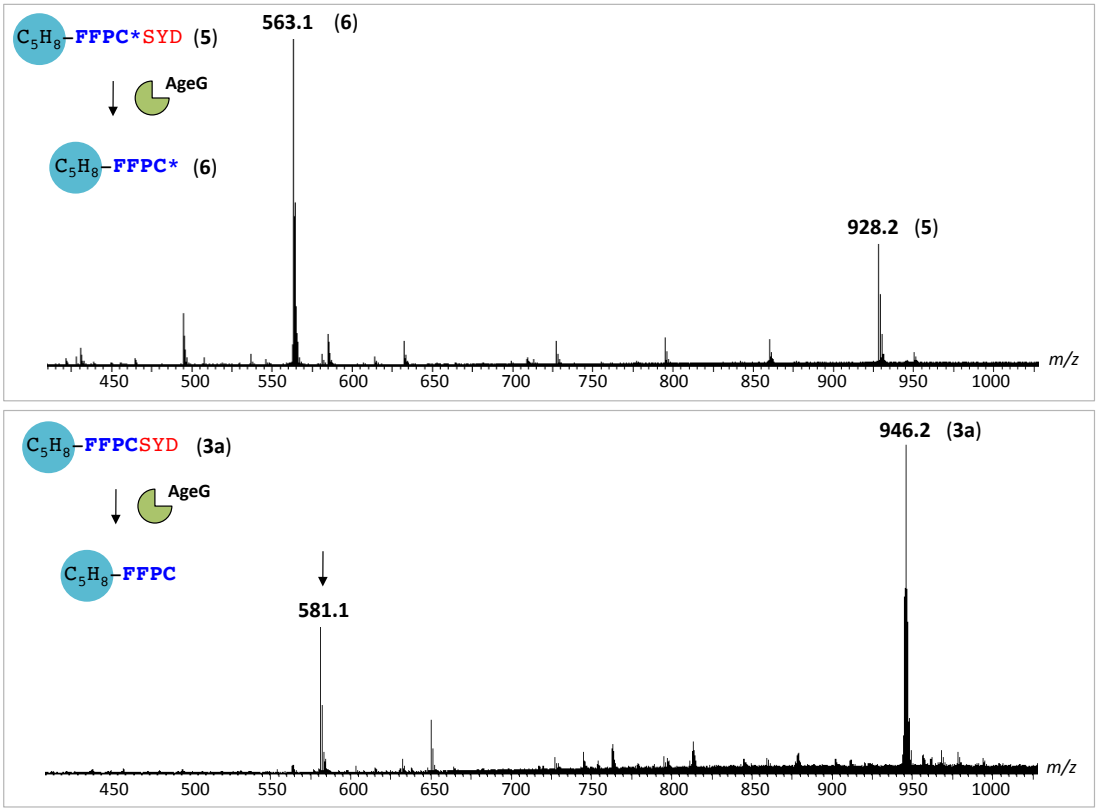

Figure S5. Substrate scope for prenylation by AgeMTPT (see Table S1). (A) Substrates (**a-j**) used in this study that were not prenylated by AgeMTPT; C* represent thiazoline. (B) Putative core sequences proposed to be substrates for homologous AgeMTPT domain from other cyanobacteria. All carry an N-terminal Phe residue, followed by a hydrophobic residue and a Pro or Cys, which is predicted to be heterocyclized. (C) Non-heterocyclized **3** was also a substrate for prenyl transfer (top), and was processed with roughly equal efficiency as the heterocyclized **4** (bottom), indicating there is a preference for the N-terminal Phe, but not the thiazoline towards the C-terminus. (D) Prenylation on the non-heterocyclic substrate does not alter downstream selectivity of AgeG, since a reaction of AgeG (5 µM) with **3a** (50 µM) in Tris buffer pH 7.5 (50 mM) and $MgCl_2$ (5 mM) at 37°C for 1 h, yielded only 20% of the proteolysed product ($[M+H]^+$ indicated by arrow, bottom) in comparison to a control reaction from route I (top), with the heterocyclized version **5** as substrate, which was converted to the expected product **6** with a yield of 64%. Moreover, proteolyzed **3a** was not a substrate for methylation.

A

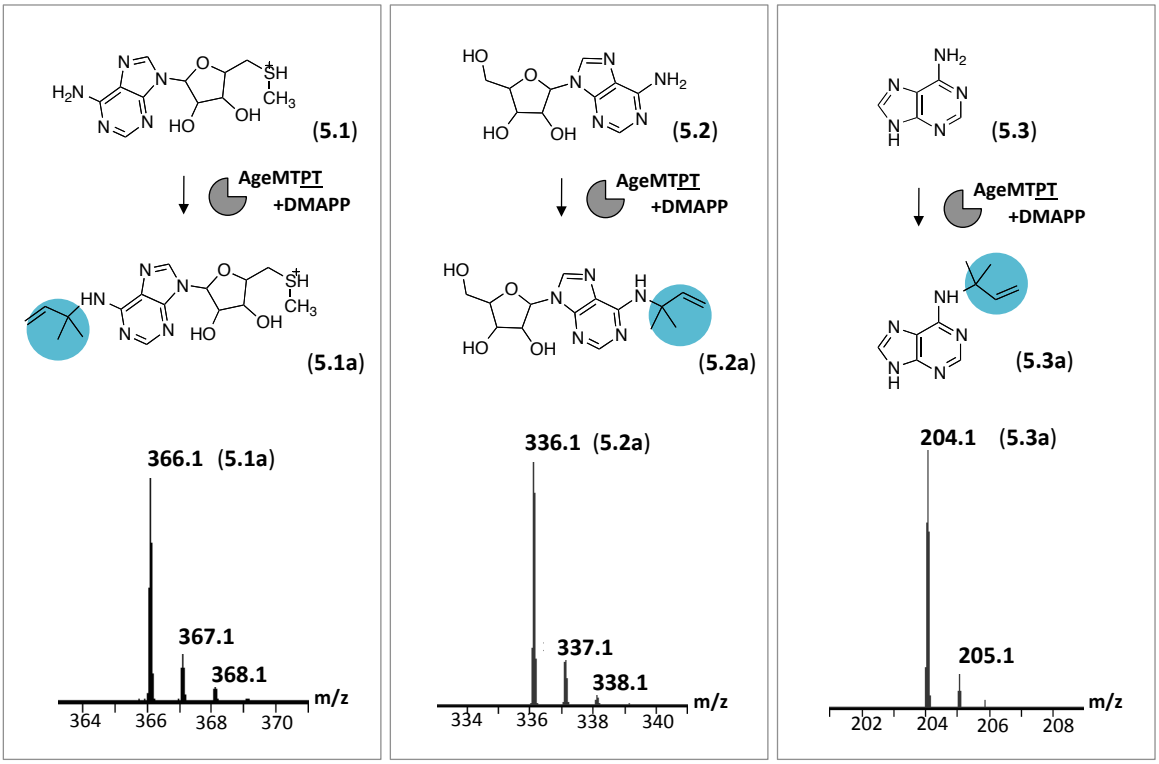
(5.1)
AgeMTPT
+DMAPP
(5.1a)
366.1 (5.1a)
367.1
368.1
m/z
364
366
368
370
(5.2)
AgeMTPT
+DMAPP
(5.2a)
336.1 (5.2a)
337.1
338.1
m/z
334
336
338
340
(5.3)
AgeMTPT
+DMAPP
(5.3a)
204.1 (5.3a)
205.1
m/z
202
204
206
208

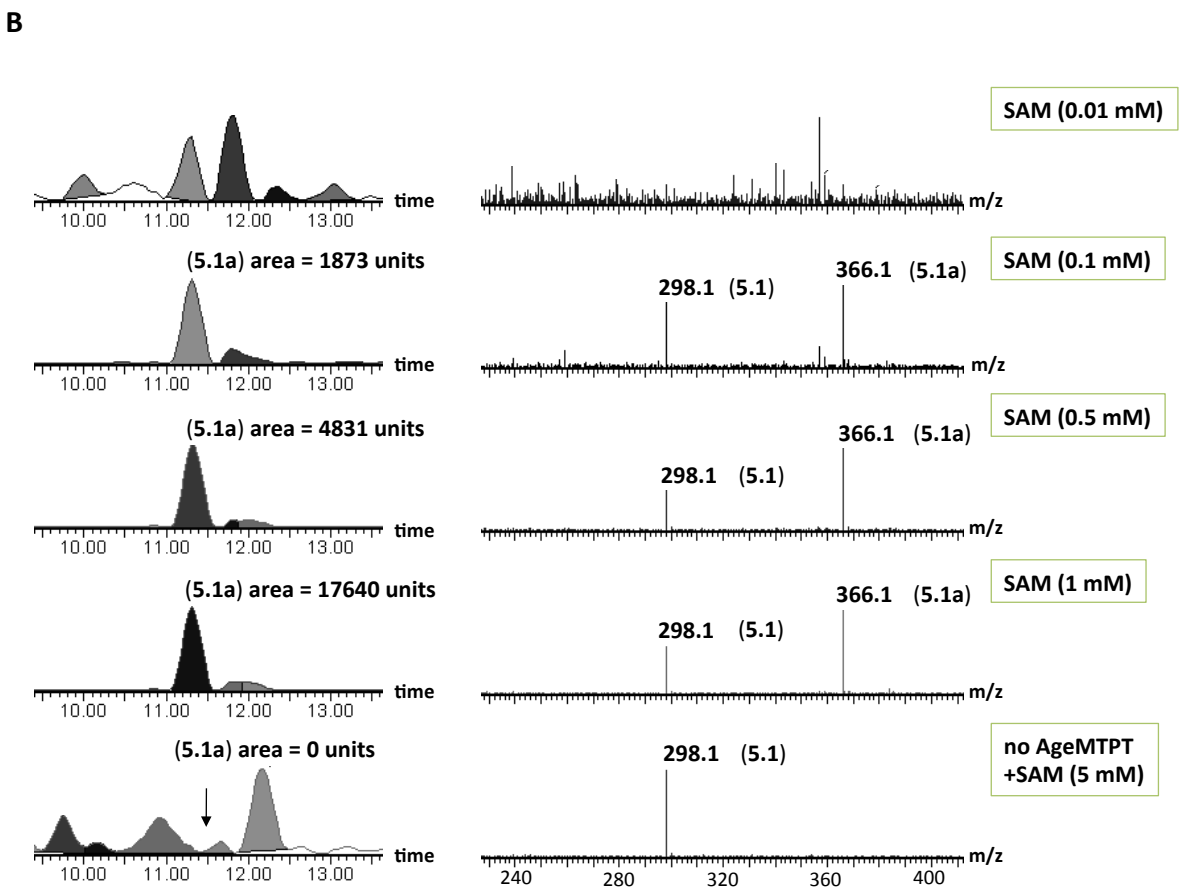

Figure S6. AgeMTPT secondary prenyltransfer reactions. Note that for products **5.1a**, **5.2a**, and **5.3a** the position of prenylation is hypothetical, and is assumed to be the free NH_2 in all cases. (A) The mass spectrum of reactions of prenylation by AgeMTPT on SAM (shown is the ionized fragment of SAM **5.1**), adenosine (**5.2**) and adenine (**5.3**). The observed SAM molecule in the mass spectrum was the fragment **5.1** with a mass of 298 Da $[M+H]^+$, corresponding to product **5.1a**. Reaction mixtures contained AgeMTPT (5 μM), DMAPP (5 mM) with substrates **5.1**, **5.2** and **5.3** (5 mM) in Tris buffer pH 7.5 (50 mM) and $MgCl_2$ (5 mM) at 37°C for 18 h. In all cases, negative control reactions were performed in absence of DMAPP. (B) Prenylation on SAM by AgeMTPT is directly proportional to SAM concentration. Reactions were done in the same conditions as in (A), but with varying SAM concentrations (0.01-1 mM, top to bottom). The area of integrated chromatograms of the product **5.1a** is shown on the left, and was found to increase proportionally to SAM. A negative control reaction in absence of AgeMTPT is shown at the bottom.

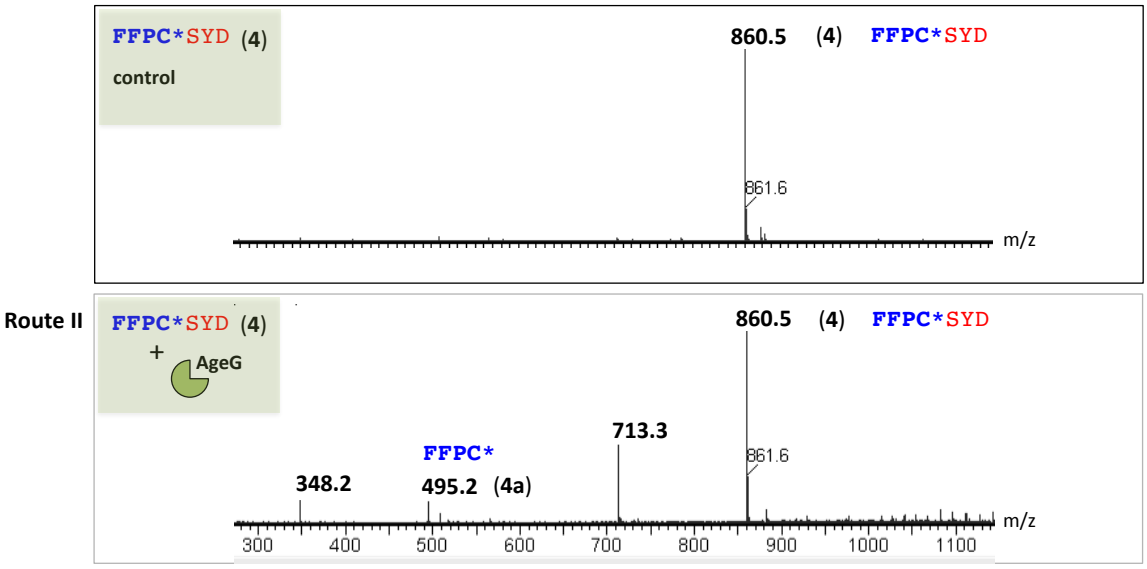

Figure S7. Fate of **4** through route II. Bottom: the mass spectrum of **4** with AgeG (10 μM), Tris buffer pH 7.5 (50 mM) and $MgCl_2$ (5 mM) at 37°C for 2 h, leading to only a minor amount of the expected proteolysed product **4a**, compared to a control reaction before addition of AgeG (top). The additional mass peak of $[M+H]^+$ 713.3 Da was also present in control reactions in absence of AgeG, and correspond to degradation product of **4** without the N-terminal Phe residue, FPC*SYD. The peak of 348.2 Da corresponds to **4a** without the first Phe residue, FPC*, and it could either be a degradation product of **4a** or a possible side-product of AgeG on the species with mass $[M+H]^+$ 713.3 Da.

A

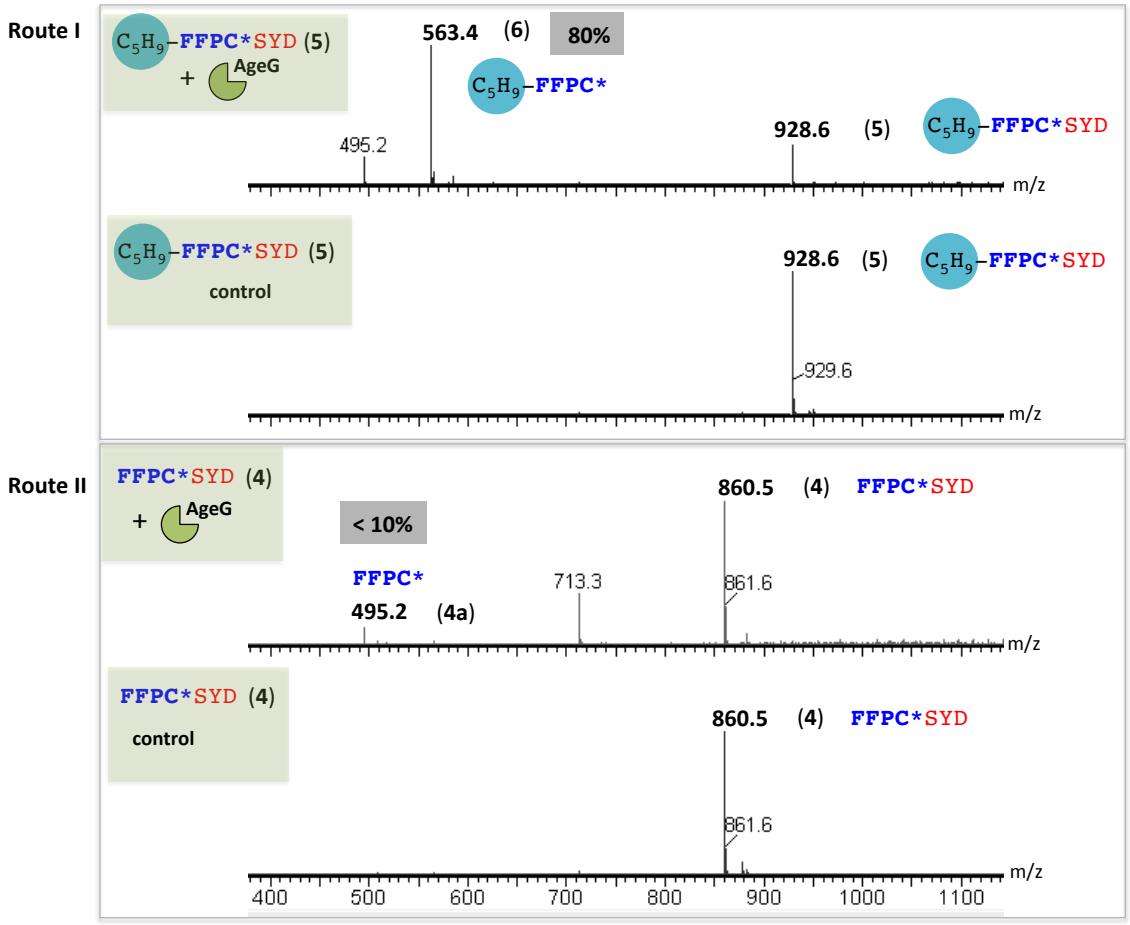
Route I
C5H9–FFPC*SYD (5)
+ AgeG
563.4 (6) 80%
C5H9–FFPC*
928.6 (5) C5H9–FFPC*SYD
495.2
m/z
C5H9–FFPC*SYD (5)
control
928.6 (5) C5H9–FFPC*SYD
929.6
m/z
Route II
FFPC*SYD (4)
+ AgeG
< 10%
860.5 (4) FFPC*SYD
FFPC*
495.2 (4a)
713.3
861.6
m/z
FFPC*SYD (4)
control
860.5 (4) FFPC*SYD
861.6
m/z
400 500 600 700 800 900 1000 1100

B

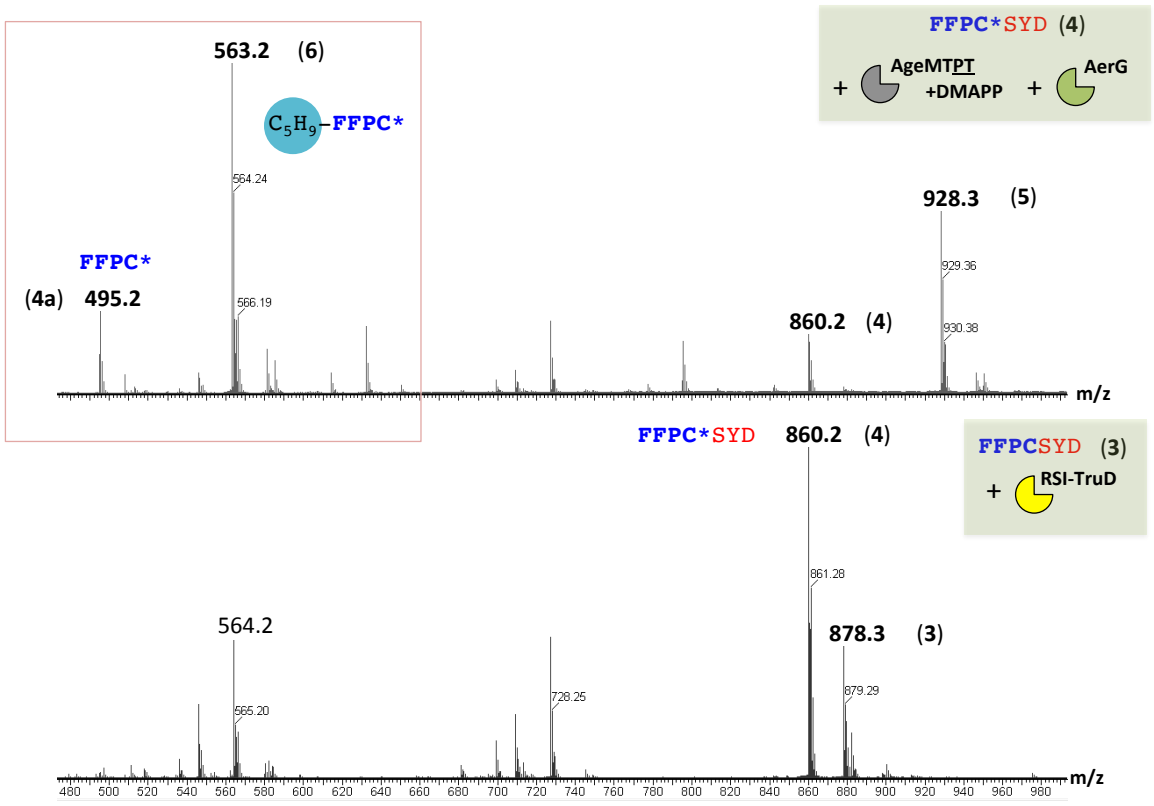

Figure S8. Compound **4** is processed through route I: (A) Side-by-side comparison of AgeG reactions on **4** (route II, bottom) and **5** (route I, top). AgeG efficiently proteolyzes the prenylated **5** to product **6**, whereas AgeG inefficiently proteolyzes **4** to the expected product **4a**. Reaction mixtures contained substrate (50 µM), AgeG (5 µM) in Tris buffer pH 7.5 (50 mM) and $MgCl_2$ (5 mM) at 37°C for 2 h. The reaction yield (%) of **4a** and **6** are given in grey boxes. (B) Competition between AgeMTPT and AgeG (1:10) on substrate **4** in a single tube. Substrate **3** was reacted with RSI-TruD to produce heterocyclized product **4** (bottom), which upon simultaneous addition of both AgeMTPT/DMAPP and AgeG leads to **6** as the major product (top). Even in excess of AgeG, the AgeMTPT route I-derived product **5** was observed, showing that the major pathway is route I. Reaction mixtures contained **3** (50 µM), AgeMTPT (1 µM), DMAPP (5 mM), AgeG (10 µM) in Tris buffer pH 7.5 (50 mM) and $MgCl_2$ (5 mM) at 37°C for 2 h.

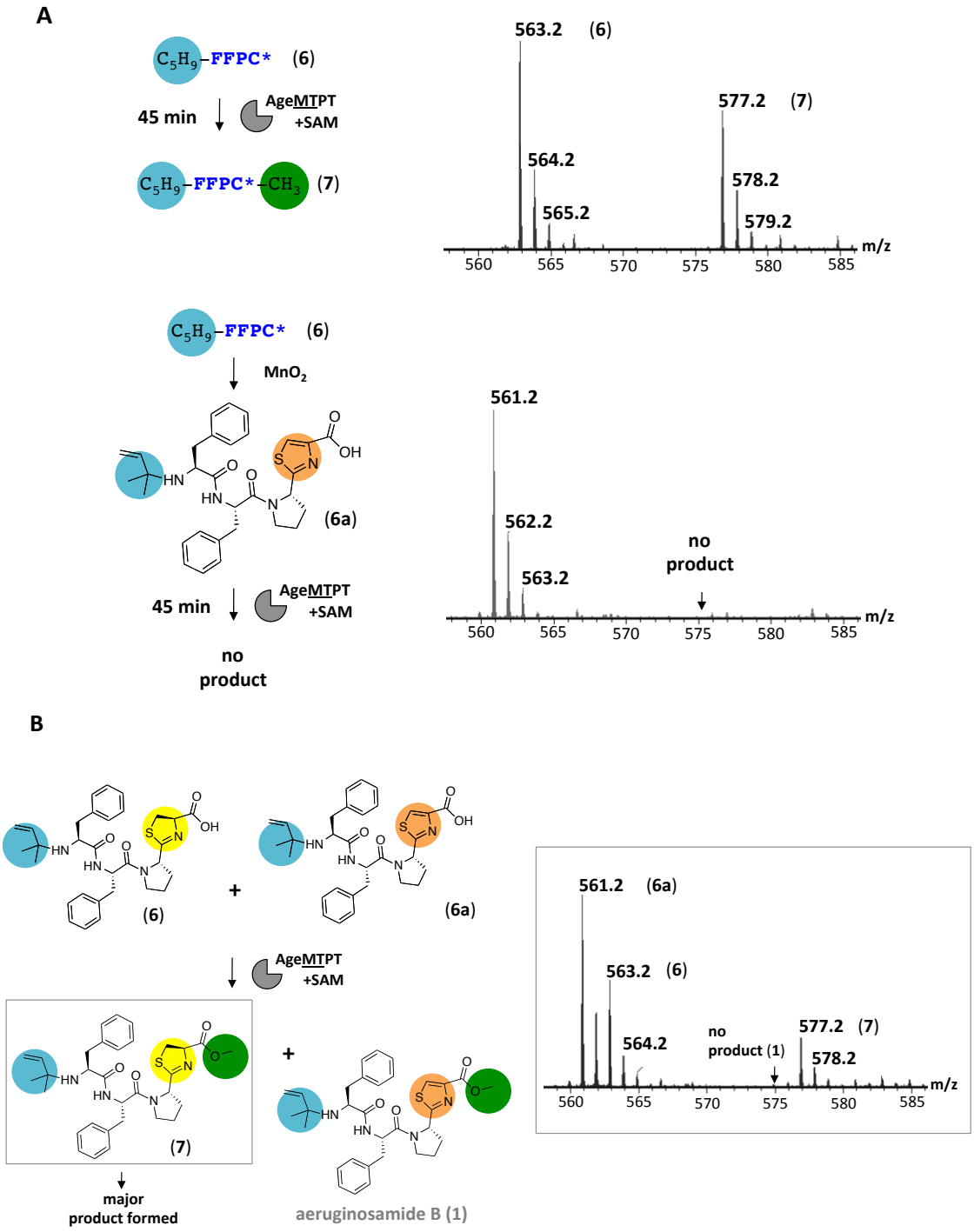

Figure S9. Specificity of AgeMTPT methylation reaction. (A) AgeMTPT methylation of substrates **6** (top) and **6a** (bottom), which was obtained by MnO_2 oxidation of **6**. AgeMTPT methylated the thiazoline in **6**, but thiazole in **6a** was not a substrate. (B) A competition reaction of AgeMTPT with a mixture of **6** and **6a** led to methylation of **6** only (to product **7**) and no reaction on **6a**. Reaction mixtures contained substrates **6** or **6a** (50 µM), AerMTPT (5 µM), SAM (5 mM) in Tris pH 7.5 (50 mM) and $MgCl_2$ (5 mM) at 37°C for 45 m.

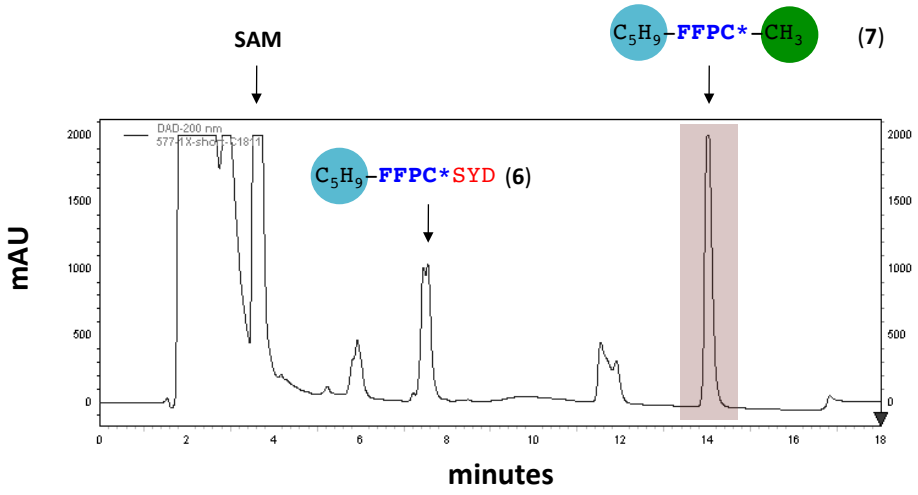

Figure S10. HPLC chromatogram of a large-scale reaction leading to **7**, which was further purified and subjected to NMR spectroscopy (see Figure S12).

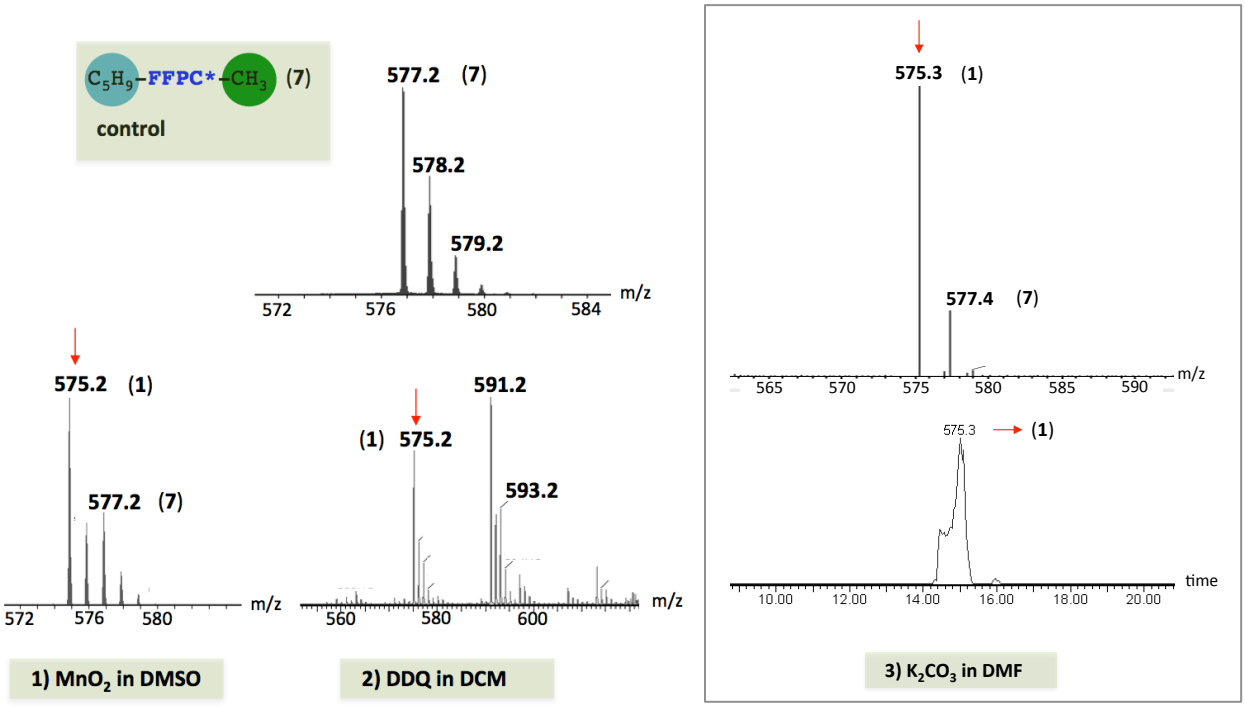

Figure S11. Oxidation of **7** to **1** by three different methods. 1) MnO_2 in DMSO. 2) DDQ in DCM. 3) The best reaction was obtained using K_2CO_3 in DMF (right, grey box), where the reaction goes to >90% completion as shown in the HPLC-ESI-MS chromatogram (bottom), and yet **1** was not stable upon isolation. Red arrows show the formation of the oxidized product **1**.

A

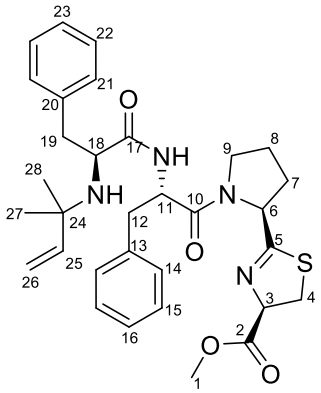

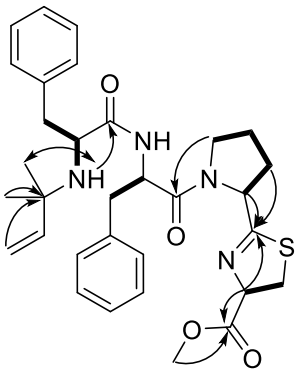

Conformer 1 (major) Conformer 2 (minor)

B

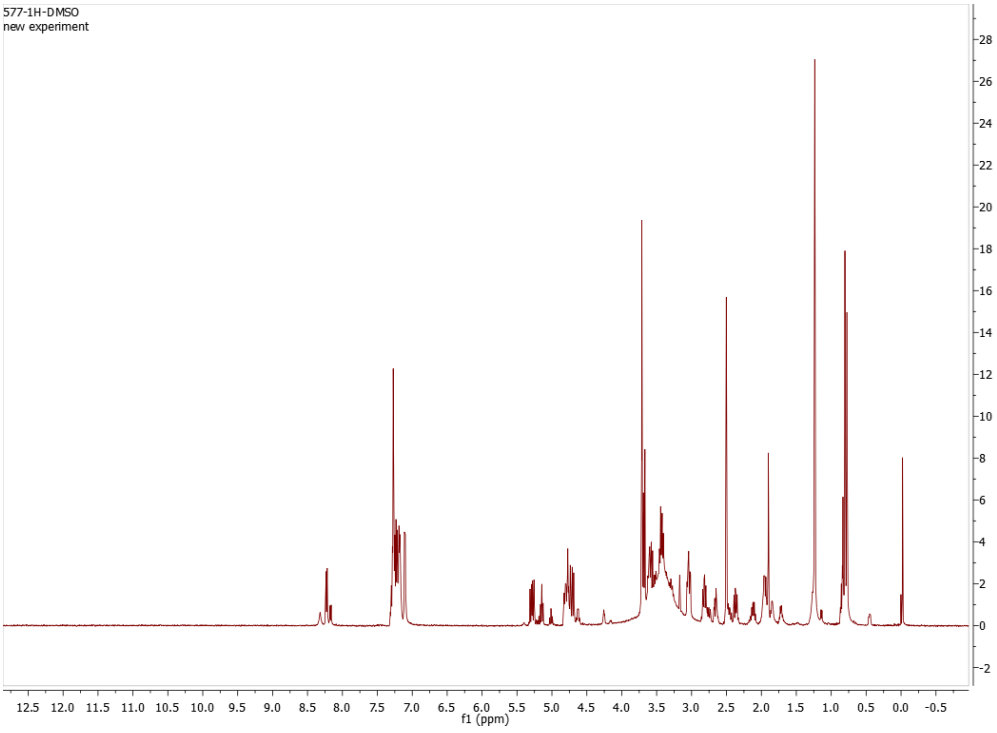

C

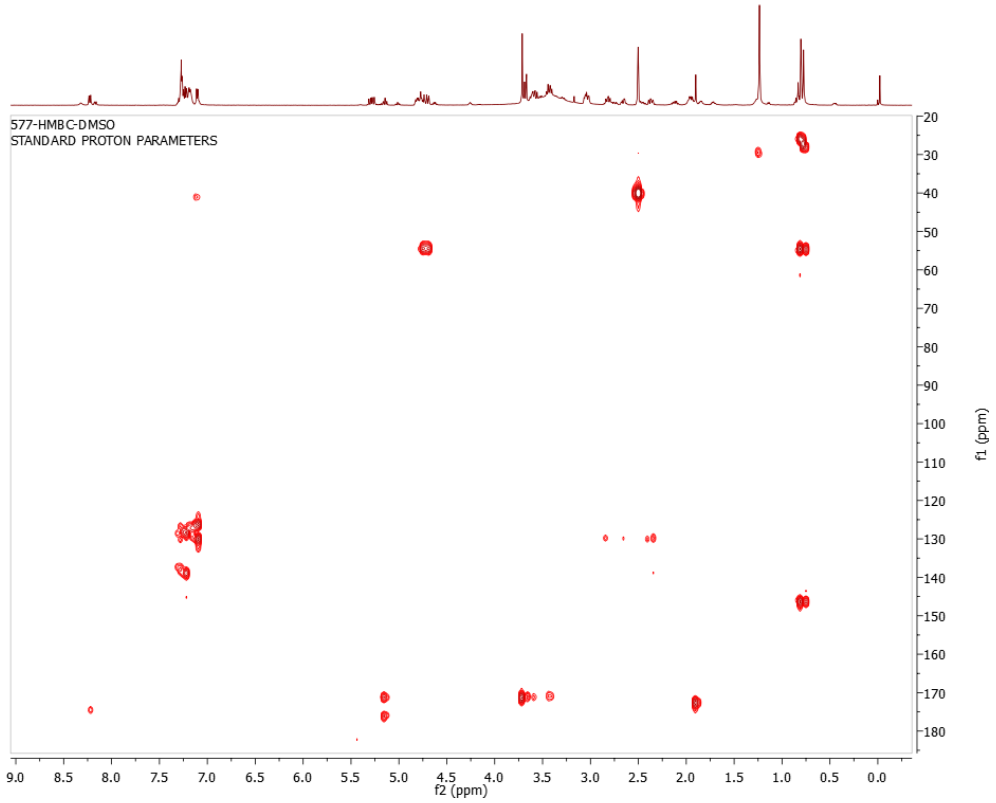
577-HMBC-DMSO
STANDARD PROTON PARAMETERS
f2 (ppm)
f1 (ppm)

D

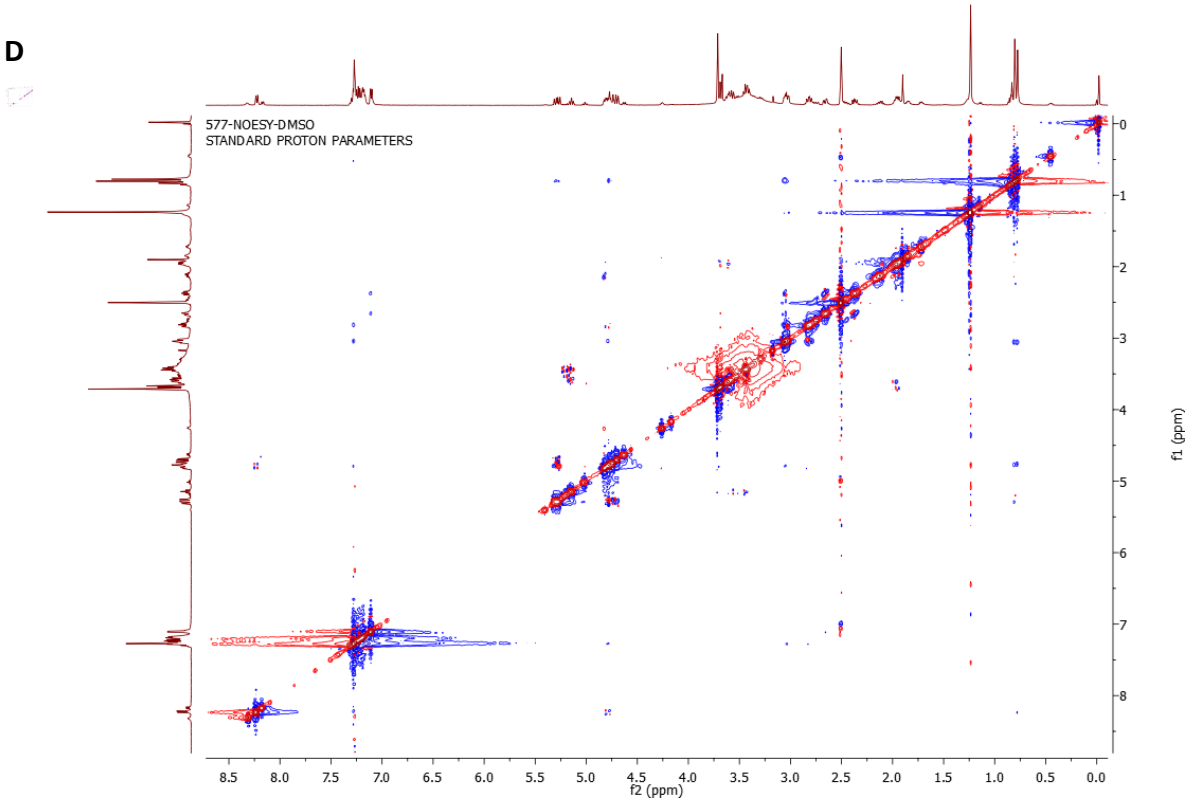
577-NOESY-DMSO
STANDARD PROTON PARAMETERS
f2 (ppm)
f1 (ppm)

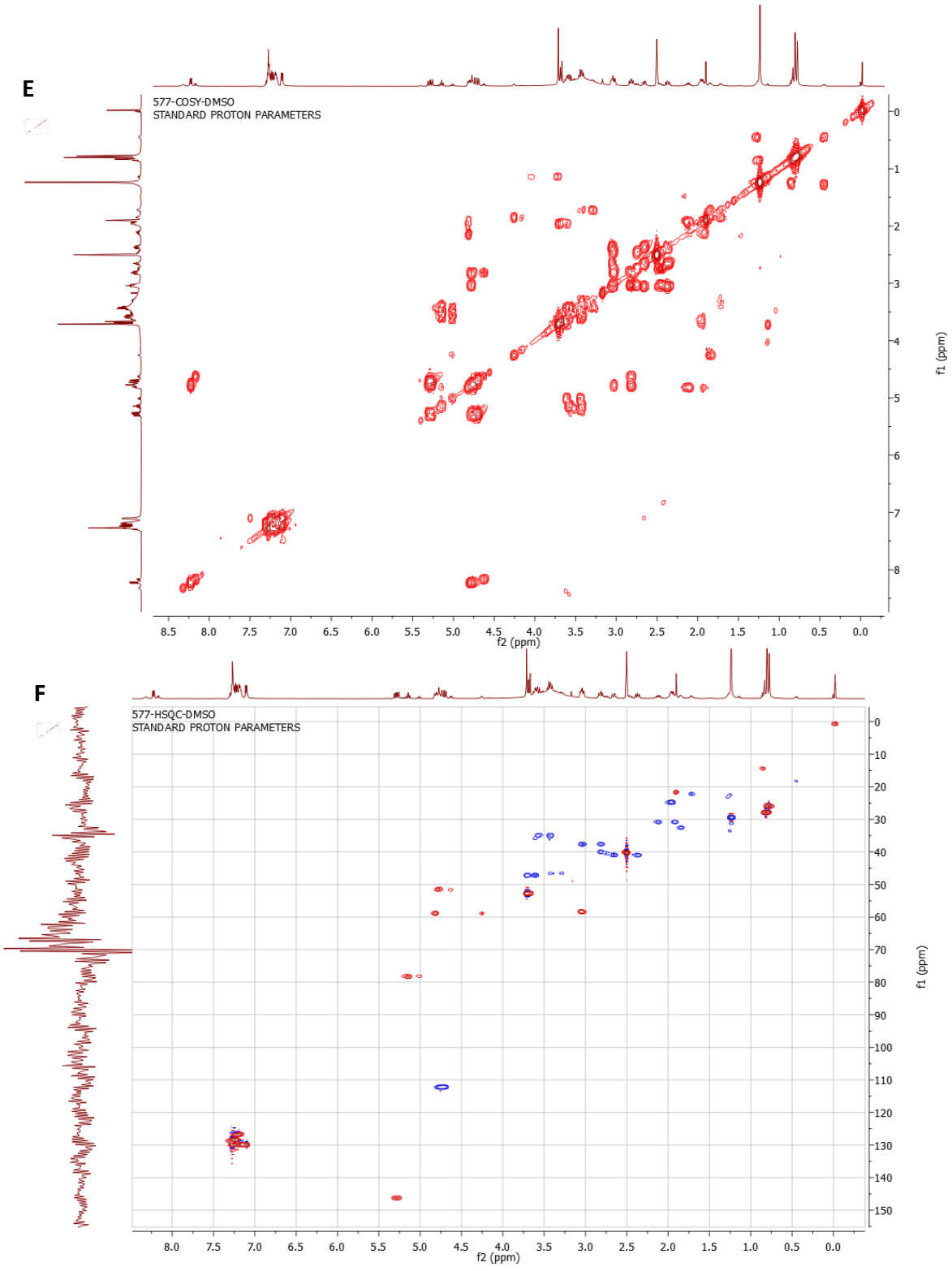

Figure S12. NMR spectra of product **7**. (A) Two conformers of **7**. (B) ^{1}H, (C) HMBC, (D) NOESY, (E) COSY, and (F) HSQC spectra of **7**. See Table S3 for tabular interpretation of data.

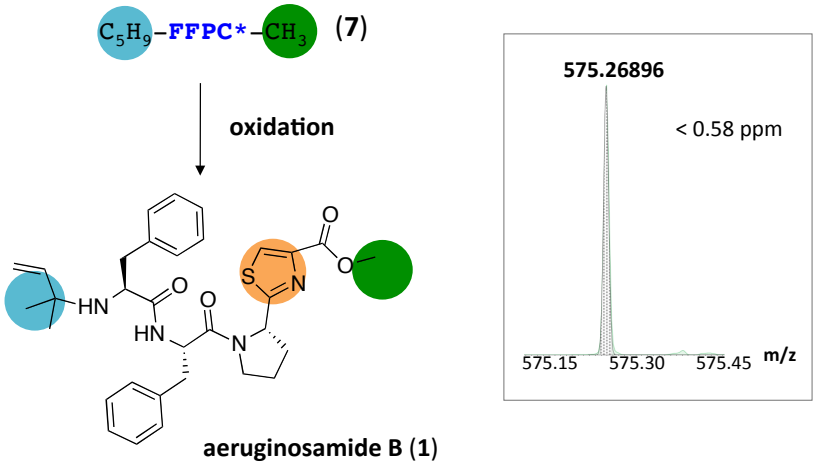

Figure S13. HRMS of **1**. Calculated for $C_{32}H_{39}N_4O_4S$, 575.26865.

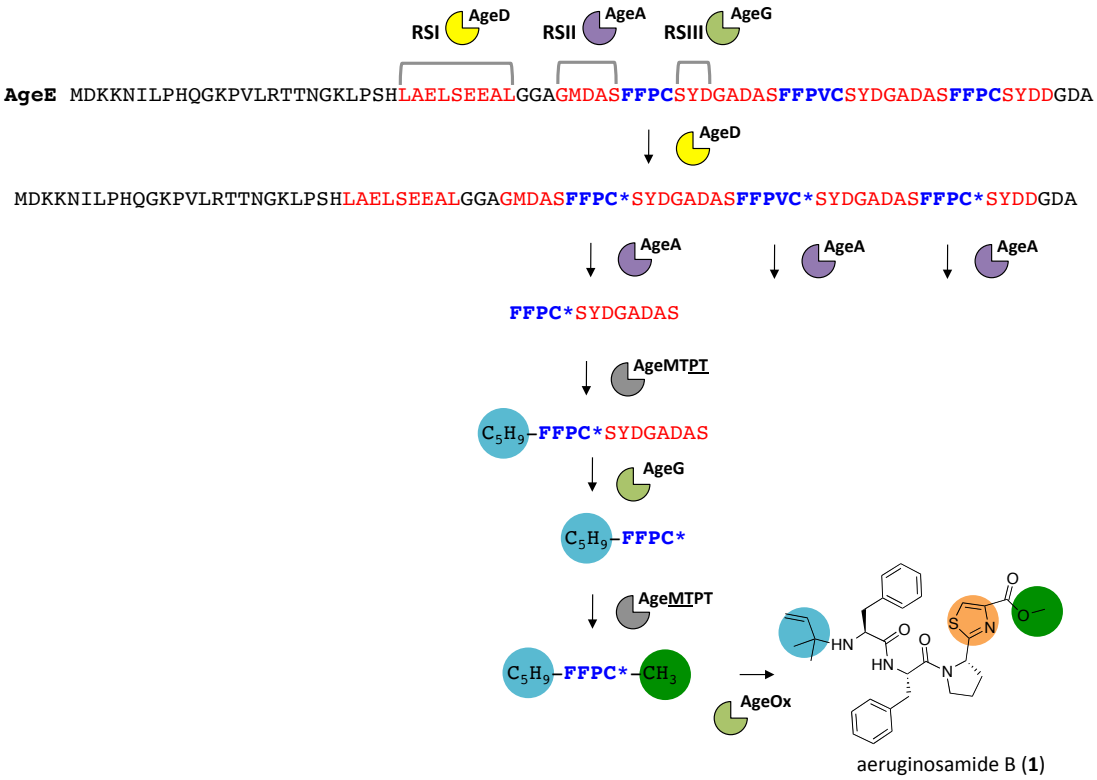

Figure S14. Proposed biosynthesis of aeruginosamide B (**1**). AgeE is the precursor peptide carrying the core (blue) encoding sequence of **1**, and proposed recognition sequences RSI-RSIII for the posttranslational enzymes AgeD, AgeA and AgeG, respectively. AgeD introduces thiazolines (C*) in core Cys, AgeA proteolyzes the N-terminus of the core, AgeMTPT prenylates the free N-terminus of the core, AgeG. proteolyzes RSIII from C-terminus of core, AgeMTPT methylates the released C-terminus of core, followed by AgeOx oxidation to thiazole, to yield the final natural product **1**.

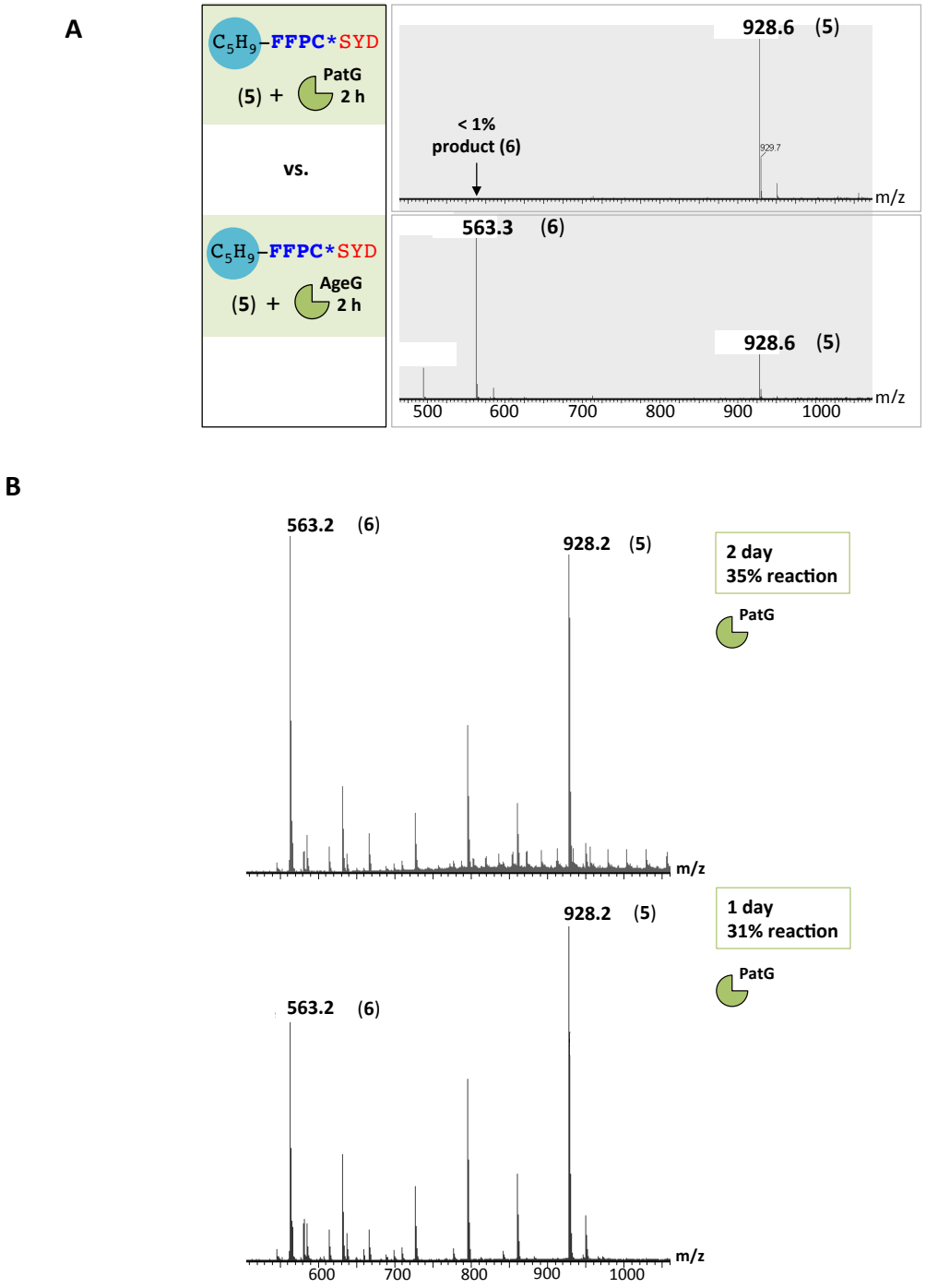

Figure S15. Comparison of reaction of PatG and AgeG on **5**. (A) In 2 h, PatG proteolyzes **5** to <1% to product, whereas AgeG proteolyzes **5** to 80% to product **6**. (B) The same reaction of **5** with PatG does not reach >35% completion even after a prolonged time-scale of 2 d. Reaction mixtures contained substrates (50 µM), PatG (10 µM) or AgeG (5 µM) in Tris pH 7.5 (50 mM) and $MgCl_2$ (5 mM) at 37°C.

Figure S16. Alignment of AgeG and PatG protease domains. In blue are the protease domains, defined by previous biochemical and structural studies.[2, 8] The canonical Ser-His-Asp catalytic triad is highlighted in red. The helical cap, present in the G family proteases but not in most subtilisin-like proteases, is shown in green.[8, 9]

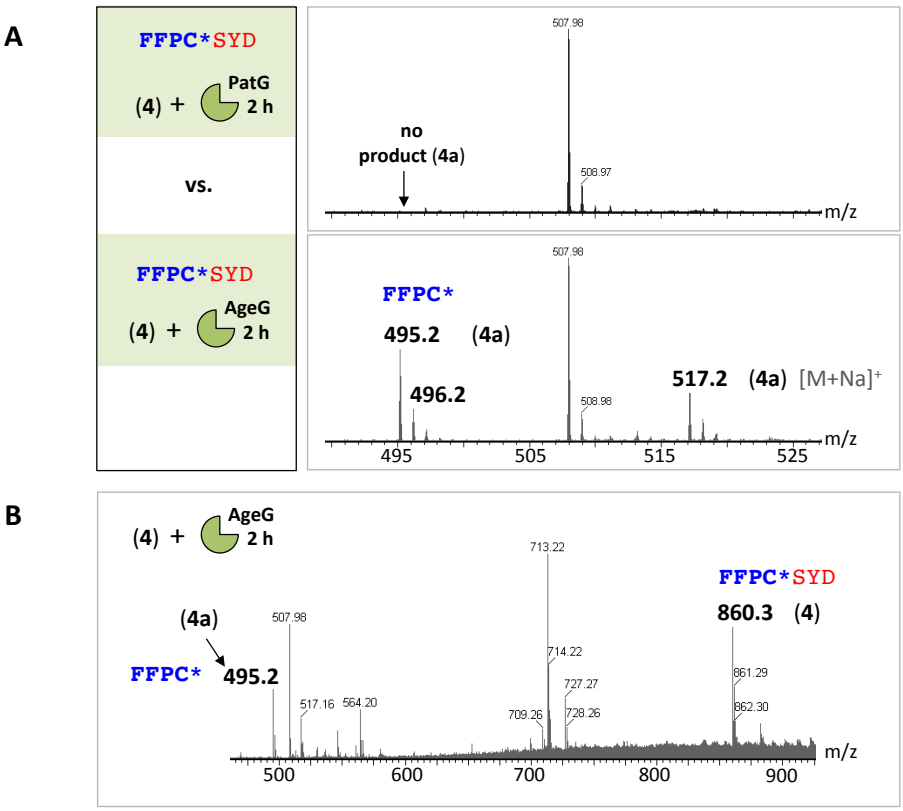

Figure S17. Comparison of reactions of PatG and AgeG on **4**. (A) The proteolysis product **4a** was not observed in reactions of **4** with PatG, but was detected in reaction with AgeG, as shown in mass spectra of **4a** $[M+H]^+$ and $[M+Na]^+$ of 495.2 Da and 517.2 Da, respectively. (B) Full spectrum of the reaction of AgeG with **4**. Reaction mixtures contained substrates (50 μM), PatG (10 μM) or AgeG (5 μM) in Tris pH 7.5 (50 mM) and $MgCl_2$ (5 mM) at 37°C for 2 h.

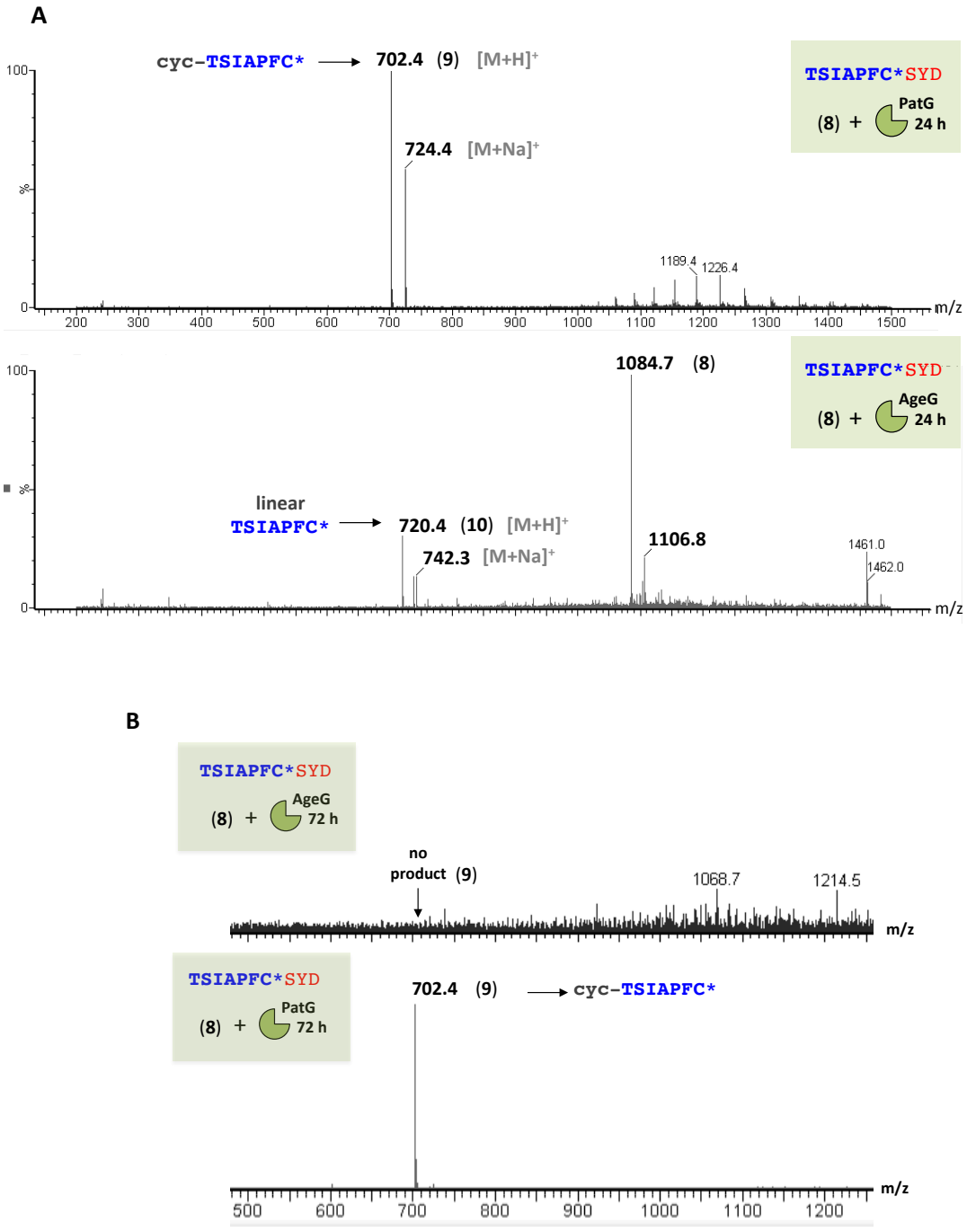

Figure S18. Comparison of reactions of PatG and AgeG on **8**. (A) Expansion of spectral data from the experiment series shown in Figure 3. (B) A specific search for **9**, 702.4 Da $[M+H]^+$ in the chromatogram shows that while PatG could cyclize **8**, AgeG could not even after a prolonged timescale of 72 h. Reaction mixtures contained substrates (50 µM), PatG (10 µM) or AgeG (10 µM) in Tris pH 7.5 (50 mM) and $MgCl_2$ (5 mM) at 37°C.

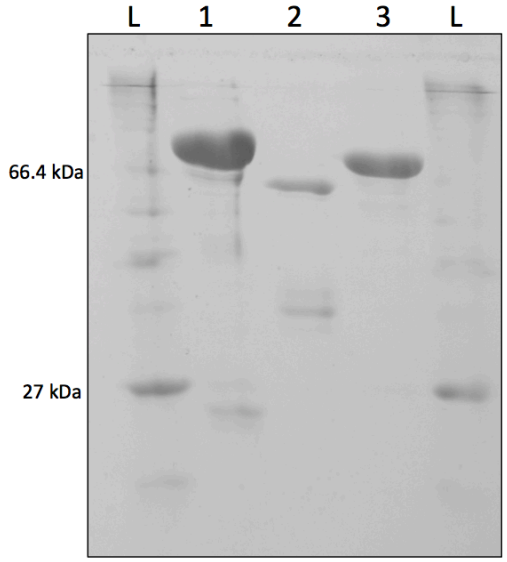

Figure S19. SDS-PAGE of proteins synthesized in this study. Ladder (L), purified RSI-TruD (lane 1), AgeMTPT (lane 2), and AgeG (lane 3).

SUPPORTING REFERENCES

(1) McIntosh, J.A.; Donia, M. S.; Schmidt, E. W. *J. Am. Chem. Soc.* **2010**, *132*, 4089.
(2) McIntosh, J. A.; Robertson, C. R.; Agarwal, V.; Nair, S. K.; Bulaj, G.; Schmidt, E. W. *J. Am. Chem. Soc.* **2010**, *132*, 15499.
(3) Sardar, D.; Lin, Z.; Schmidt, E. W. *Cell Chem. Biol.* **2015**, *22*, 907.
(4) McIntosh, J. A.; Donia, M. S.; Nair, S. K.; Schmidt, E. W. *J. Am. Chem. Soc.* **2011**, *133*, 13698.
(5) Ishihara, H.; Shimura, K. *FEBS Lett.* **1987**, *226*, 319.
(6) Li, X.; Li, C.; Yin, B.; Li, C.; Liu, P.; Li, J.; Shi, Z. *Chem. Asian J.* **2013**, 8, 1408.
(7) Huang, Y.; Gan, H.; Li, S.; Xu, J.; Wu, X.; Yao, H. *Tet. Lett.* **2010**, *51*, 1751.
(8) Agarwal, V.; Pierce, E.; McIntosh, J.; Schmidt, E. W.; Nair, S. K. *Cell Chem. Biol.* **2012**, *19*, 1411.
(9) Koehnke, J.; Bent, A.; Houssen, W. E.; Zollman, D.; Morawitz, F.; Shirran, S.; Vendome, J.; Nneoyiebge, A. F.; Trembleau, L.; Botting, C. H.; Smith, M. C.; Jaspars, M.; Naismith, J. H. *Nat. Struct. Mol. Biol.* **2012**, *19*, 767.